

CLARA-A2: The second edition of the CM SAF cloud and radiation data record from 34 years of global AVHRR data

K.-G. Karlsson¹, K. Anttila², J. Trentmann³, M. Stengel³, J.F. Meirink⁴, A. Devasthale¹, T. Hanschmann³, S. Kothe³, E. Jääskeläinen², J. Sedlar¹, N. Benas⁴, G.-J. van Zadelhoff⁴, C. Schlundt³, D. Stein³, S. Finkensieper³, N. Håkansson¹ and R. Hollmann³

[1]{Swedish Meteorological and Hydrological Institute (SMHI), Norrköping, Sweden}

[2]{Finnish Meteorological Institute (FMI), Helsinki, Finland}

[3]{Deutscher Wetterdienst (DWD), Offenbach, Germany}

[4]{Royal Netherlands Meteorological Institute (KNMI), De Bilt, The Netherlands}

Correspondence to: K.-G. Karlsson (Karl-Goran.Karlsson@smhi.se)

Abstract

The second edition of the satellite-derived climate data record CLARA (“The CM SAF cLoud, Albedo and surface RAdition dataset from AVHRR data” - second edition denoted CLARA-A2) is described. The data record covers the 34-year period from 1982 until 2015 and consists of cloud, surface albedo and surface radiation budget products derived from the AVHRR (Advanced Very High Resolution Radiometer) sensor carried by polar-orbiting, operational meteorological satellites. The data record is produced by the EUMETSAT Climate Monitoring Satellite Application Facility (CM SAF) project as part of the operational ground segment. Its upgraded content and methodology improvements since edition 1 are described in detail as well as some major validation results. Some of the main improvements of the data record come from a major effort in cleaning and homogenising the basic AVHRR level 1 radiance record and a systematic use of CALIPSO-CALIOP cloud information for development and validation purposes. Examples of applications studying decadal changes in ArcticPolar sSummer surface albedo and cloud conditions, as well as global cloud redistribution patterns, are provided.

1 Introduction

Global distribution of cloudiness and existing cloud feedback on the radiative forcing continue to be important topics in climate research. Uncertainties in the description and understanding of both topics are considered to be dominant in explaining the spread among climate models in their prediction of current and anticipated climate

1 change (Webb et al., 2013; Vial et al., 2013). In parallel, better knowledge and monitoring of global cloudiness
2 and radiation are also required for a successful increased utilisation of renewable energy sources, such as solar
3 power plants (Šúri et al., 2007). In order to address requests and challenges in these and adjacent fields by a
4 systematic utilization of satellite measurements, the Climate Monitoring Satellite Application Facility (CM SAF)
5 was formed by the European Organisation for the Exploitation of Meteorological Satellites EUMETSAT (Schulz
6 et al., 2009).

7 CM SAF (www.cmsaf.eu) aims at developing capabilities for a sustained generation and provision of Climate
8 Data Records (CDRs) derived from operational meteorological satellites. The ultimate aim is to make the
9 resulting data records suitable for the analysis of climate variability and the detection of climate trends.
10 Examples of important guidelines for the compilation of CDRs are, (1) to apply the highest standards and
11 guidelines as ~~lined out~~lined by the Global Climate Observing System (GCOS), (2) to process satellite data within
12 a true international collaboration benefiting from developments at international level and, (3) to perform
13 intensive validation and improvement of the CM SAF CDRs, including a major role in data record assessments
14 performed by research organizations such as the World Climate Research Programme (WCRP).

15 One of CM SAF's CDRs is CLARA: "The CM SAF cLoud, Albedo and surface RAdiation dataset from
16 AVHRR data". It is based on data from the Advanced Very High Resolution Radiometer (AVHRR) operated
17 onboard ~~the~~ polar orbiting NOAA satellites as well as by the MetOp polar orbiters operated by EUMETSAT
18 since 2006. AVHRR offers one of the longest satellite observation records, with its first measurements ~~starting~~
19 ~~commencing already~~ in 1978. The first edition of CLARA (CLARA-A1) was released in 2012 and is described
20 by Karlsson et al., (2013). This paper describes improvements and other features of the second edition, CLARA-
21 A2, which was released in 2017~~6~~.

22 The basic AVHRR radiance measurements were previously described in detail by Karlsson et al. (2013).
23 Consequently, Section 2 describes only the extension of the data series since CLARA-A1 and some further
24 modifications to improve calibration and homogenisation of the entire data record. Section 3 includes general
25 descriptions on how the data record was compiled and Sections 4 ~~through~~ -6 explain the most significant
26 improvements made to retrieval methods for the three different groups of parameters (clouds, surface albedo and
27 radiation) together with some validation results. For the latter, some focus has been on extensive inter-
28 comparisons being made to space-borne active lidar cloud retrievals (CALIPSO-CALIOP) and to other existing
29 satellite-based data records (e.g., PATMOS-x and MODIS). Section 7 discusses potential applications and
30 provides some examples of analyses possible ~~from with~~ a continuous, homogeneous 34-yr data record. Finally,
31 Section 8 summarises the main features of the data record and presents future plans.

32

33 2 Extension and homogenisation of the historic AVHRR data record

34 The basic AVHRR radiance measurements (level 1 observations) used in CLARA-A2 are described in detail by
35 Karlsson et al. (2013). However, the temporal coverage is now extended with six additional years (2010-2015)
36 resulting in a total length of 34 years (1982-2015). Figure 1 illustrates all satellites and their respective
37 measurements periods for the CLARA-A2 climate data record. ~~From this figure it~~ It is clear that the observational
38 coverage varies considerably: ~~there is~~ only one satellite in orbit providing measurements during the 1980s and

1 | early 90s, ~~until~~ while during the last decade ~~where~~ at least four simultaneous satellites were present (with a
2 | peak of 6 satellites available simultaneously in 2009). ~~Additionally~~Further, orbital drift for individual satellites,
3 | lead~~ing~~ to changing local observation times and this, ~~contributes to create to rather~~ varying observational
4 | conditions during the period. However, some sub-setting of the data could still yield relatively homogeneous
5 | observation conditions. For example, ~~if~~ choosing exclusively afternoon satellites (which is possible with the
6 | CLARA-A2 data record) a quite homogeneous and stable time series of observations can be achieved.

7 | The AVHRR instrument was initially built for operational global weather monitoring purposes, not for climate
8 | monitoring. This means that the radiometric accuracy and the stability of radiance measurements are sometimes
9 | problematic for some early satellites in the time series. In addition, NOAA archiving of data has its own
10 | problems with ~~spurious~~ intermittent occurrences of gaps, duplications and corrupt data, depending on time
11 | period and satellite. Consequently, a substantial effort in the preparation of CLARA-A2 has been made to correct
12 | and homogenize the entire radiance (level 1) record. A special pre-processing tool (PyGAC) was developed for
13 | these purposes, described in detail by Devasthale et al. (2016). Some of the most important aspects have been the
14 | following:

- 15 | - Removal of corrupt data
- 16 | - Data rescue of data with incorrect header definitions
- 17 | - Removal of duplicated orbits
- 18 | - Removal of overlap between orbits
- 19 | - Homogenization of visible calibration by removal of trends and performing inter-calibration
20 | techniques between satellites (based on the method by Heidinger et al. (2010), but extended with
21 | more satellites and with MODIS Collection 6 as reference data)
- 22 | - Improving accuracy of infrared calibration (compared to CLARA-A1) by using a more accurate
23 | treatment of calibration target data
- 24 | - Applying median filters to AVHRR channel 3b (at 3.7 microns) brightness temperatures for reducing
25 | the impact of high noise levels for satellites NOAA-7 to NOAA-14
- 26 | - Removal of partially corrupt orbits in periods with AVHRR scan motor problems (primarily between
27 | years 2001-2005; this was mostly based on manual inspection efforts since operational data flagging
28 | does not sufficiently cover this problem ~~sufficiently well~~)

29 | The overall impact of these ~~measures~~ treatments resulted in the exclusion of approximately 6 % of all original
30 | level 1 data in the NOAA archive from processing. The work with improving the AVHRR level 1 data record (or
31 | the Fundamental Climate Data Record – FCDR) has been performed within the framework of the WMO project
32 | SCOPE-CM (<http://www.scope-cm.org/>) ~~and~~ and the ESA Cloud_cci project (http://www.esa-cloud_cci.org).

34 | 3 Product overview highlighting changes in product aggregation since CLARA-A1

35 | The CLARA-A2 CDR is based on instantaneous AVHRR Global Area Coverage (GAC) retrievals (i.e., for
36 | every orbit at approximately 4 km horizontal swath resolution in nadir) which have been aggregated to derive the
37 | final spatio-temporally averaged data records. Since CLARA-A1, an important change for the cloud products is

Ändrad fältkod

Formaterat:
Standardstycketeckensnitt,
Teckensnitt:12 pt, Tyska (Tyskland)

Formaterat:
Standardstycketeckensnitt,
Teckensnitt:12 pt, Tyska (Tyskland)

1 the introduction of globally resampled daily composites (level-2b) as the basis for computation of final level-3
2 products. The level-2b data representation (introduced by Heidinger et al., 2014) is motivated by the
3 inhomogeneous global coverage of polar sun-synchronous satellite data. Each polar satellite offers around 14
4 evenly-distributed observations per day for each location near the poles, ~~while when passing at~~ the equator, each
5 location is observed only twice, approximately 12 hours apart. The ~~idea with the introduction purpose~~ of the
6 level-2b data representation is to form a more homogeneous data record having only two observations at the
7 most nadir-viewing angle per day per satellite for each location globally. The alternative ~~to of using~~ all
8 available observations for Level-3 products (as was done for CLARA-A1) results in a ~~very~~-skewed distribution
9 of the observations because of the inhomogeneous observation frequency (increasing with latitude). By selecting
10 only the observations which are made closest to the nadir condition, we ensure that observations are made at
11 almost the same viewing conditions and, most importantly, observations are made at nearly the same local time
12 globally for each level-2b product.

13 The level-2b approach leads to a significant reduction of the amount of used observations. However, the high
14 observation frequency near the poles is undoubtedly very valuable, and, consequently, there are also separate
15 polar products added which are based on all available observations. The level-2b approach is used exclusively
16 for cloud products and not for surface radiation and surface albedo products where the use of all existing data is
17 more critical.

18 Final level 3 cloud products are available as daily and monthly composites where the monthly means are
19 computed from daily means. Results are defined for each satellite on a regular latitude/longitude grid with a
20 spatial resolution of $0.25^\circ \times 0.25^\circ$ degrees. In addition, results for cloud amount as well as the surface albedo
21 (see Section 5) are available on two equal-area polar grids at 25 km resolution for the Arctic and Antarctic
22 regions, respectively; these grids are centred at the poles and cover areas of approximately 9000 km x 9000 km.
23 The new features for CLARA-A2 include the availability of all daily level-2b products and a demonstration data
24 record of probabilistic cloud masks (further explained in the next section).

25 Monthly averages of cloud products are also available in aggregated form (i.e., merging all satellites).
26 Acknowledging the different observation capabilities during night and during day, and also taking existing
27 diurnal variations in cloudiness into consideration, a further separation of ~~data-some~~ products into exclusive day
28 and night portions has been performed as a complement to the standard products based on all data. ~~Her~~For these
29 complementary productse, all observations made under twilight conditions (solar zenith angles (SZA) between
30 75° - 95°) have been excluded in order to avoid being affected by specific cloud detection problems occurring in the
31 twilight zone (e.g. Derrien and LeGleau, 2010).

32 All products described in the following three sections are described in detail in Product User Manuals (PUM),
33 Algorithm Theoretical Basis Documents (ATBD) and Validation reports (VAL), all available via the CM SAF
34 web user interface (accessible from www.cmsaf.eu). These documents are important as they describe and
35 reference the latest algorithms utilized in the processing of the CLARA-A2 data record; the peer-reviewed
36 publications of retrieval algorithms referred to in the following Sections 4-6 may not always be up-to-date with
37 these very latest algorithm changes.

38

1
2
3
4
5
6
7
8
9
10
11
12
13
14
15
16
17
18
19
20
21
22
23
24
25
26
27
28
29
30
31
32
33
34
35
36

4 Cloud products

A list of all CLARA-A2 aggregated cloud products is given in Table 1. These products have been derived from the pixel-level retrievals of the respective cloud properties, which are also made available in the form of level-2b products, as outlined in Section 3. Basic methods for deriving these parameters ~~were already introduced~~ can be found in by Karlsson et al. (2013). Consequently, the following sub-sections only provide a brief introduction to the products, list the most significant improvements since CLARA-A1 and introduce some new features.

4.1 Improvements of basic cloud products derived from the NWCSAF cloud processing package

The Cloud Fractional Cover (CFC) product is derived directly from results of a cloud screening, or cloud masking, method. CFC for one particular instantaneous observation is defined as the fraction of cloudy pixels per grid box compared to the total number of analysed pixels ~~in the~~ within that grid box, expressed ~~in~~ as percent. This product is calculated using the NWC SAF Polar Platform System (PPS) cloud processing software (Dybbroe et al., 2005). CFC is also prepared in complementary daytime and nighttime conditions. The PPS method also computes the Cloud Top level (CTO) product, providing the cloud top level as geometrical height, cloud top pressure ~~or~~ and cloud top temperature. The CTO retrieval ~~is using~~ uses two different radiance matching methods, one for clouds identified as opaque and one for semi-transparent clouds.

CLARA-A2 takes advantage of some significant upgrades of the cloud masking and CTO retrievals in the latest PPS version. ~~Regarding improvements~~ Generally, -of cloud masking, the utilisation of reference measurements from the CALIPSO-CALIOP sensor (Winker et al., 2009, Vaughan et al., 2009) has been fundamental for the development and validation of the methods, following approaches by Karlsson and Dybbroe (2010) and Karlsson and Johansson (2013). The most important improvements regarding cloud screening include the following:

- PPS dynamic cloud masking thresholds have been adjusted, -guided by cloud optical thickness information provided by CALIPSO-CALIOP, to detect a larger fraction of the thinnest clouds. Thus, thresholds for AVHRR visible reflectances and infrared brightness temperature differences (the latter often sensitive to presence of semi-transparent clouds) have been optimized.
- Identification of thin and fractional clouds over ocean surfaces has been improved by adding two new image feature tests: 1. Analysis of warmest pixels in a local neighbourhood. 2. Credibility tests of Sea Surface Temperature (SST) estimates based on standard SST retrieval schemes.
- and to better account for variations in New dynamic thresholds for infrared brightness temperature differences features have been introduced, in particular for the differences relative to the 3.7 micron channel over arid and semi-arid regions. For CLARA-A1 some static thresholds were used previously which led to occasional false cloudiness and unrealistic cloud distributions and trends over semi-arid regions as reported by Sun et al., (2015) and Sanchez-Lorenzo et. al., (2017). The new thresholds are functions of surface emissivities (from MODIS climatologies) /reflectivities and viewing angles in arid and semi-arid regions. The impact of these changes is illustrated in Fig. 2 showing changes

Formaterat: Teckensnitt:10 pt

Formaterat: Teckensnitt:10 pt

Formaterat: Liststycke, Punktlista +
Nivå: 1 + Justerad vid: 0,63 cm +
Indrag vid: 1,27 cm

Formaterat: Teckensnitt:10 pt

Formaterat: Teckensnitt:10 pt

Formaterat: Teckensnitt:10 pt

Formaterat: Teckensnitt:10 pt

Formaterat: Teckensnitt:10 pt

Formaterat: Teckensnitt:10 pt

1 between CLARA-A1 and CLARA-A2 over the African continent. Clear reductions are shown over
2 semi-arid regions while for other regions changes are close to neutral or slightly positive.

3 ~~- The challenging cloud screening conditions near the poles have also received special attention. Cloud~~
4 ~~detection during pPolar day conditions over snow- and ice-covered surfaces has been optimised, and~~
5 ~~falsely detected clouds during pPolar night conditions have been largely removed. In both cases the~~
6 ~~access to CALIOP cloud masks and CALIOP-estimated cloud optical thicknesses has been extremely~~
7 ~~valuable. Various validation scores have been studied and PPS thresholds were adjusted to optimise the~~
8 ~~scores. The latter removal of falsely detected clouds unfortunately leads to a systematic and enhanced~~
9 ~~(compared to CLARA-A1) underestimation of cloudiness over the Arctic and Antarctic regionsa during~~
10 ~~the pPolar night. However, we are of the opinion that this better reflects the true cloud detection~~
11 ~~limitations of the AVHRR sensor in situations with very cold ground temperatures than for compared to~~
12 ~~the previous case with spuriously frequently occurring false cloudiness in cold situations.~~

13 Figure 32 compares results from CLARA-A1 and CLARA-A2 using global, synoptic surface observations
14 (SYNOP) of cloud cover. For this study, the CLARA-A2 monthly mean product, generated from all available
15 satellites, was compared against SYNOP monthly mean cloud cover calculated based on daily means. Only those
16 stations and months where at least 6 observations per day for 20 days of the respective month were included in
17 the comparison (see the VAL report for more details). Results show relatively small changes in CFC bias but a
18 substantial decrease in the bias-corrected root mean squared error (bc-RMSE) for CLARA-A2. Thus, a much
19 better agreement with the SYNOP observed variability in cloud cover is achieved. The relatively unchanged bias
20 reflects inherent and unavoidable differences in the viewing geometry for the two observation types.

21 The improvements in cloud detection are also reflected in comparisons with cloud observations from the
22 CALIPSO-CALIOP instrument. Karlsson and Johansson (2013) compared CLARA-A1 results with CALIPSO-
23 CALIOP data for 99 selected NOAA-18 orbits and we have repeated this study for CLARA-A2 with overall
24 global results provided in Tab. 2: the validation scores (bias, Kuipers and Hitrate) are explained in Karlsson and
25 Johansson (2013). The number of matched field of views (FOVs) differs slightly here despite using the same 99
26 matched orbits which is explained by some pixels being masked out for quality reasons (in the polar areas) in the
27 CLARA-A1 data record. We notice that more clouds are detected (bias being reduced) in CLARA-A2 despite
28 the fact that some previous false classifications over semi-arid regions are now removed. Thus, both more clouds
29 are detected and the cloudy/cloud-free separation has improved, indicated by improved Kuipers and Hitrate
30 scores.

31 Figures 43 and 54 demonstrate the achievements made in cloud detection efficiency in CLARA-A2 in much
32 more detail. Results are based on an extensive cloud product monitoring effort utilising near-simultaneous (i.e.,
33 within 3 minutes) observations from the CALIPSO-CALIOP sensor over almost-nearly ten years (2006-2015).
34 Despite the nadir-only observation capability of the CALIOP sensor compared to the wide-swath coverage from
35 AVHRR, it has been possible to collect a global picture of cloud detection efficiency by accumulating results
36 over the relatively long time period. Figure 43 shows the global overall frequency of correct cloudy and cloud-
37 free estimations (referred to as Hitrate). In this figure we have only considered CALIOP-detected clouds with
38 vertically integrated optical depths exceeding 0.15 (thinner clouds being treated as cloud-free cases). This is
39 done to avoid being overly influenced by the presence of sub-visible clouds (explaining a large part of the

Formaterat: Teckensnitt:10 pt

Formaterat: Teckensnitt:10 pt

Formaterat: Teckensnitt:10 pt

Formaterat: Teckensnitt:10 pt

Formaterat: Teckensnitt:10 pt

Formaterat: Teckensnitt:10 pt

Formaterat: Teckensnitt:10 pt

Formaterat: Teckensnitt:10 pt

Formaterat: Teckensnitt:10 pt

Formaterat: Teckensnitt:10 pt

Formaterat: Teckensnitt:10 pt

Formaterat: Teckensnitt:10 pt

Formaterat: Teckensnitt:10 pt

Formaterat: Teckensnitt:10 pt

1 | negative bias values in Tab. 2) beyond detection capability in passive imagery. Results show a general global
2 | agreement in cloud screening well above 80 % apart from over the poles and high-latitude land areas and over
3 | high mountainous terrain. Decreased Hitrates are also found over the marine dry sub-tropical regions near the
4 | climatological centres of sub-tropical highs. We suspect that ~~but~~ this is mainly attributed to increasing
5 | geolocation mismatches between AVHRR- and CALIOP-observed clouds frequently-being present on the
6 | AVHRR GAC sub-pixel scale (less than 4 km). In other words, true small-scale or fractional clouds may exist in
7 | any of the two inter-compared data records but not always simultaneously in both because of the small sizes of
8 | cloud elements. These mismatches increase when facing conditions having a larger proportion of sub-AVHRR
9 | pixel scale cloudiness and such conditions are likely to occur in the central regions of the marine sub-tropical
10 | highs. Here we encounter more scattered cloudiness, occurring either as individual cumulus clouds or as broken
11 | stratocumulus or cumulus clouds in open cell formation (as described by Stevens et al., 2005) while away from
12 | these regions clouds organize more frequently as closed cells or as extensive stratocumulus cloud decks. Cases
13 | with a more dominant appearance of small cumulus and/or fractional stratocumulus can also occur over land
14 | surfaces but the more heterogenic conditions over land are likely to create a more diversified distribution of
15 | cumulus clouds in different stages of development and size. Nevertheless, the lower Hitrates also observed over
16 | the eastern part of South-America and in eastern Africa may also be explained by a high frequency of sub-pixel
17 | scale cloudiness.

18 | ~~More serious is the somewhat~~The poorer results seen over regions where cold surface conditions may prevail for
19 | considerable portions of the year (Fig. 4) is a potentially more serious issue. Figure 54 exemplifies this by
20 | showing the probability of detecting cloudy conditions over the Arctic. Over the coldest portions of Greenland
21 | and the inner Arctic, almost 50 % of the clouds remain undetected in CLARA-A2 during the polar winter. On the
22 | other hand, cloud screening complications are reduced during the polar summer when results are nearly as good
23 | as over any other region on Earth (excluding some highly elevated areas of Greenland).

24 | Comparisons have also been made to the MODIS (Moderate Resolution Imaging Spectroradiometer) sensor
25 | Collection 6 data record (http://modis-atmos.gsfc.nasa.gov/products_C006update.html) from the Aqua satellite
26 | (Fig. ~~ure~~ 65). Generally, we find a very good agreement between the two data records, both in the geographical
27 | distribution and in the zonal averages, of global cloud conditions for the overlapping data records of 2002-2014.
28 | There is a bias of about 5 % in cloud cover (MODIS higher) which-that is relatively constant over all latitudes
29 | (Fig. ~~ure~~ 65, lower panels). This increased d cloudiness in clouds in MODIS data is interpreted as representing the
30 | improvements in spectral channel availability of the MODIS sensor in comparison to AVHRR. However, the
31 | very good correlation with MODIS results is encouraging considering the availability of two more decades of
32 | results from AVHRR.

33 | CLARA-A2 also includes a demonstration data record of probabilistic cloud masking following Karlsson et al.
34 | (2015), defined in the level 2b data record. The alternative formulation here provides a measure of uncertainty in
35 | cloud masking for the user to consult, compared to the traditional binary cloud mask utilized when compiling
36 | level 3 CFC products. The intention is to shift entirely to a probabilistic formulation in the third edition of
37 | CLARA planned for release in 2021.

1 The CTO retrieval in CLARA-A2 has been subject to several minor modifications while retaining the same
2 principle methodology. However, the most significant improvement is related to an optimisation of the iterative
3 procedure leading to a substantial efficiency leap regarding the fraction of resulting valid retrievals. The previous
4 method in CLARA-A1 was not able to provide valid estimations for all semi-transparent clouds, where only
5 approximately which resulted in that only about 70 % of all cloudy cases got yielded valid CTO retrievals. The
6 new PPS version used in CLARA-A2 processing provides CTO estimations for more than 97 % of all cases.
7 This is especially important for the joint cloud-histogram product (JCH, see Section 3.3) and its ability to reflect
8 true climatological conditions. The improvement has resulted from applying more physically sound constraints
9 to the iterations (i.e., seeking the best physically reasonable solution instead of seeking the best solution and
10 discarding it if it's not physically reasonable).

12 **4.2 Cloud products derived from the CM SAF Cloud Physical Properties (CPP) package**

13 The CPP products include cloud thermodynamic phase (CPH), cloud optical thickness (COT), particle effective
14 radius (REF) and liquid/ice water path (LWP/IWP). Since 2012, the CPP package is included in the NWC SAF
15 PPS cloud processing package. CPH is determined from a cloud typing approach following Pavolonis et al.
16 (2005). This cloud type algorithm consists of a series of spectral tests applied to infrared brightness
17 temperatures. It has a night-time branch, as well as a daytime branch in which shortwave reflectances are also
18 considered. COT and REF are retrieved using the classical Nakajima and King (1990) approach, which is based
19 on the principle that cloud reflectance is mainly dependent on COT at a non-absorbing, visible wavelength and
20 on REF at an absorbing, near-infrared wavelength. In the CPP algorithm (Stengel et al., 2014; Roebeling et al.,
21 2006), the Doubling-Adding KNMI (DAK, De Haan et al., 1987; Stammes, 2001) radiative transfer model
22 (~~RTM~~) is used to simulate visible (0.6 μm) and near-infrared (1.6/3.7 μm) TOA reflectances as a function of
23 viewing geometry, COT, REF, and CPH. These simulated reflectances are stored in a look-up table (LUT) and
24 satellite-observed reflectances are matched to this LUT in an iterative manner, leading to the derivation of COT
25 and REF. These two parameters are then used to compute LWP and IWP, as in Stephens (1978). Uncertainty
26 estimates of the CPP products are also derived and provided.

27 Major updates compared to the CPP version applied for CLARA-A1 (Karlsson et al., 2013) include the
28 implementation of the new cloud phase algorithm in the NWC SAF PPS software package (first made in PPS
29 version 2012 and for the latest improvements in PPS version 2014), the generation of improved cloud reflectance
30 LUTs, and the inclusion of observational sea ice (OSI SAF, 2016) and ERA-Interim reanalysis (Dee et al., 2009)
31 numerical weather prediction (NWP) snow cover data to better characterize the surface albedo. It should be
32 noted that, since CPP retrievals require reflectances from shortwave channels, CPP products, besides apart from
33 CPH, are available exclusively during daytime (i.e., not during twilight and night). Since CPH is retrieved both
34 during night and day, a complementary CPH(day) product is also provided.

35 Figure 76 shows the CPH, LWP and IWP products averaged over the 5-year period 2003-2007. Large scale
36 climatological characteristics of clouds are apparent, including the marine stratocumulus regions off the west
37 coasts of the continents, the Inter-Tropical Convergence Zone (ITCZ), consisting mainly of ice clouds, and the

1 | mid-latitude cyclone tracks ~~on-in~~ both hemispheres. High cloud water path values over polar regions should be
2 | largely attributed to inadequate retrievals over snow- and ice-covered surfaces, providing little contrast with
3 | clouds in the AVHRR visible channel.

4 | Inter-comparison efforts with other similar data records show a generally agreement better than 5 % for CPH
5 | (i.e. for absolute frequencies of water clouds) and 0.005 kg m⁻² for LWP and IWP, although the bias compared to
6 | DARDAR IWP is larger. More details on these results can be found in the VAL report.

7 | Further illustrations of LWP and IWP results are given in Figs ~~87~~ and ~~98~~. Figure ~~8a7~~ shows the monthly time
8 | series of LWP in the ~~t~~ Tropics from CLARA-A2, along with ~~CLARA-A1 and~~ two other satellite-based data
9 | records. Between them, PATMOS-x is the most similar to CLARA-A2, since it covers the same period and was
10 | based on the same (AVHRR) measurements. MODIS, on the other hand, covers the last 12 years of the time
11 | series and is the most stable, since it involves a single (here: MODIS on Aqua is used), well-calibrated
12 | instrument. In general, the LWP records agree well in terms of ~~seasonal variability (see also the bottom panel of~~
13 | ~~Fig. 7) and~~ absolute amount of tropical LWP, ~~except for a large bias in the case of CLARA-A1 (Fig. 8a).~~
14 | ~~However, an improvement is apparent from CLARA-A1 to CLARA-A2, with the latter showing better~~
15 | ~~agreement with PATMOS-x and MODIS. This difference between CLARA-A1 and CLARA-A2 is attributed~~
16 | ~~mainly to changes in CPH, due to the implementation of a new retrieval algorithm. In terms of seasonal~~
17 | ~~variability, all data records agree well, and differences between the two CLARA editions are minor (Fig. 8b).~~
18 | Both CLARA-A2 and PATMOS-x show some trends during various parts of the time series, which ~~should beare~~
19 | ~~largely-primarily~~ attributed to orbital drift.

20 | It should also be noted that during the period 01/2001-05/2003, channel 3a of AVHRR onboard NOAA-16 was
21 | switched on and used for the retrievals, instead of channel 3b, which was used throughout the rest of the time
22 | series. This switch causes a jump in the time series of both CLARA-A2 and PATMOS-x. Comparisons of LWP
23 | were also made against an independent, microwave-based data record (O'Dell et al., 2008), focusing on the main
24 | stratocumulus regions, where liquid clouds prevail (not shown). Results showed good agreement in both the
25 | seasonal cycle and absolute values of LWP, with an average bias of -0.0034 kg m⁻², fluctuating in the range
26 | ±0.01 kg m⁻². Furthermore, Fig. ~~98~~ shows a validation of pixel-level CLARA-A2 IWP with Cloudsat-CALIOP-
27 | based DARDAR observations (Delanoë and Hogan, 2008). An overall underestimation by CLARA-A2 is
28 | observed, which becomes larger at high IWP values. Further analysis indicates that this disagreement is mainly
29 | caused by differences in REF (especially for thick clouds), while COT agrees well between the two data records
30 | (not shown).

31 | 4.3 Multi-parameter cloud product representations

32 | The joint cloud property histogram (JCH) product is a combined histogram of CTP and COT covering the
33 | solution space of both parameters (e.g., Rossow and Schiffer, 1991). This two-dimensional histogram gives the
34 | frequency of occurrences for specific COT and CTP combinations defined by a constant bin space, separable for
35 | liquid and ice clouds. This product is defined on a slightly coarser grid (1°x1° resolution) in order to achieve
36 | higher statistical significance and to maintain manageable file sizes. The product is currently archived on the
37 | grid-point resolution, so user-defined JCH analysis regions can be created.

1 Since the JCH product is a product visualisation technique, its quality is dependent on the quality of the
2 visualized products, including CTO (here, cloud top pressure), COT and CPH. Improvements of those products
3 have already been described but we repeat some of the [valid-important](#) points here:

- 4 - The increase in the number of valid CTO results gives a better representation of the true CTP-COT
5 distribution
- 6 - The histograms are now based on cloud products defined in the level-2b representation mode giving a
7 more homogeneous and consistent data distribution
- 8 - Frequencies of occurrences in each bin as well as the total cloud cover for all cases are now given
9 (although the latter can still deviate slightly from the CFC product value since for JCH we require all
10 three products - CTO, COT and CPH – to be simultaneously available).

11 Figure [109](#) shows global CLARA-A2 JCHs for afternoon satellites together with corresponding results from
12 Aqua-MODIS Collection 6_ ~~and~~ PATMOS-x [and CLARA-A1](#) over the period 2003-2014 (i.e., the Aqua-
13 MODIS era). [Notice, however, that there are no CLARA-A1 data after 2009 leading to a shorter period with data](#)
14 [\(2003-2009\) for that data record in Fig. 10](#). In comparison to global JCH results for CLARA-A1 (Karlsson et al.,
15 2013 [and bottom panels in Fig. 10](#)) we highlight that clouds are now more frequent at higher and lower
16 tropospheric levels. This agrees well with MODIS and PATMOS-x, although the latter two have more boundary
17 layer clouds present, especially over open water (Fig. [109d-i](#)).

18 Over land, MODIS and PATMOS-x distributions show an increased frequency of mid- and high-level clouds,
19 and a reduction in shallow cumulus and stratiform clouds (Fig. [109f](#), i). A relative increase in very optically thick
20 mid- and upper-level clouds, representative of nimbostratus and deep convection, also emerges for MODIS and
21 PATMOS-x. CLARA-A2 distributions generally agree with these distribution changes, although with CLARA-
22 A2 there is a tendency to observe a higher frequency of optically thinner clouds (COT ranging 0.3-3.6) across
23 the tropospheric column (Fig. [109c](#)). Furthermore, there is a substantial amount of ~~very~~ optically ~~very~~ thick mid-
24 to upper-level clouds in CLARA-A2 and PATMOS-x (Fig. [109c](#), i), which are largely absent in MODIS (Fig.
25 [109f](#)). In CLARA-A2, this feature is linked to problems in estimating COT properly over snow-covered surfaces
26 and therefore COT products over these surfaces should be treated with caution. A JCH where the Antarctic
27 continent was masked resulted in the removal of this relative peak of high COT at mid- to high cloud levels in
28 CLARA-A2 (not shown).

30 **5 The surface albedo product**

31 The cloud mask and AVHRR radiance data have been used as primary input data to generate the CLARA-A2
32 surface albedo (SAL) product of terrestrial black-sky surface albedo (wavelengths of 0.25-2.5 μm). It is available
33 as pentad (five-day) and monthly means and has the same spatial resolution and projection(~~s~~) as the other
34 CLARA-A2 products. Examples of the CLARA-A2 SAL product for January and July 2012 are given in Fig.
35 [110](#).

36 The retrieval algorithm of CLARA-A2 SAL follows the same outline as the previous CLARA-A1 SAL
37 described in detail in Riihelä et al. (2013): After cloud masking, the possible effect of topography on geolocation

1 and radiometry in locations with inclined slope is corrected. Then, for the pixels on land, a correction for
2 scattering and absorption effects of aerosols and other atmospheric constituents is performed. In CLARA-A2
3 SAL, a dynamic aerosol optical depth (AOD) time series has been used. It has been composed using the Total
4 Ozone Mapping Spectrometer (TOMS) and Ozone Monitoring Instrument (OMI) aerosol index data
5 (Jääskeläinen et al., 2016). A correction for reflectance anisotropy of vegetated surfaces and spectral albedo is
6 then calculated. In CLARA-A1, one land use classification (LUC) was used for the whole time series. For the
7 current SAL product, four different LUCs are used. Finally a narrow-to-broadband conversion is made to derive
8 the albedo over the full spectral range of the product (0.25-2.5 μm). Since the reflectance anisotropy of snow is
9 large and varies according to snow type (Peltoniemi et al., 2005), the albedo of snow and ice covered areas is
10 derived by averaging [the broadband bidirectional reflectances of the AVHRR overpasses](#) into pentad or monthly
11 means ~~the broadband bidirectional reflectances of the AVHRR overpasses~~. These overpasses are found to cover
12 the whole viewing hemisphere (SZA smaller than 70° and satellite zenith angles smaller than 60°) in most of the
13 cases, giving a good representation of the bidirectional reflectance distribution function. For the observations
14 over open water, the albedo is constructed as a function of SZA and wind speed. Wind information is taken from
15 microwave measurements (SMMR and SSM/I data) and available SYNOP observations. The classification
16 between open water and sea ice has been verified using the Ocean and Sea Ice Satellite Application Facility (OSI
17 SAF) sea ice extent data (Eastwood, 2014).

18 In summary, the main differences in the algorithm between CLARA-A1 SAL and CLARA-A2 SAL are as
19 follows:

- 20 - atmospheric correction uses dynamic AOD time series
- 21 - number of LUCs used has been increased from one to four
- 22 - wind speed data is used over sea to describe the sea surface roughness

23 The data record has been validated against in situ albedo observations from the Baseline Surface Radiation
24 Network (Ohmura et al., 1998), the Greenland Climate Network (Steffen et al, 1996), and the TARA floating ice
25 camp (Gascard et al., 2008). The sites have been chosen according to data availability, temporal coverage of
26 measurements and quality of data. The validation results show that CLARA-A2 SAL has a relative accuracy of
27 10-20 % over vegetated sites, and typically 3-15 % over snow and ice. Larger differences between the in situ
28 measurements and the satellite-based albedo value are mostly related to the heterogeneity of high-resolution
29 near-infrared surface reflectances at CLARA-A2 SAL pixel scales. The spatial representativeness is an issue at
30 most of the sites and should always be considered when using measurements of different scale (and location) for
31 validation (Riihelä et al., 2012).

32 The SAL time series was also compared to MCD43C3, the surface albedo product from MODIS (Schaaf et al.,
33 2002). The comparison showed that on a global scale, the two products are in good agreement. An overview of
34 the MODIS comparison results [for both CLARA-A2 and CLARA-A1 SAL](#) can be seen in [Figure 124](#), showing
35 the mean black sky albedo. These data have been averaged over the common retrievable land/snow area after
36 coarsening the MODIS product to 0.25° spatial resolution and averaging the CLARA-A2 SAL pentad means to fit
37 the MODIS products (delivered as 16-day means). Water areas are excluded from the analysis since the MODIS
38 product is not defined for water bodies (including sea ice areas). The ~~two CLARA-A2 and MCD43C3~~ products

1 are in good agreement and generally the albedo differences are less than 5 %, especially during the latter half of
2 2009. In general, the difference is caused by the methodology differences, where the MODIS albedo product is
3 normalized to local noon, which, for surfaces other than snow, produces the minimum daily albedo. Taking this
4 into consideration, CLARA-A2 SAL values ~~should be expected to~~ be slightly higher than the MODIS product
5 values. An analysis of the differences on latitudinal bands (not shown) shows that over the northern hemisphere,
6 the largest differences appear over Arctic land areas. The topography (which is corrected for in SAL but not in
7 the MODIS product) also creates differences in the average albedo ~~at over~~ mountainous regions. The albedo
8 values of CLARA-A2 SAL are considerably closer to MODIS albedo values than CLARA-A1 SAL values are.
9 This has been achieved by using dynamic AOD in the atmospheric correction of CLARA-A2 SAL.

10 The temporal stability of the CLARA-A2 SAL time series has also been evaluated using the central part of the
11 Greenland ice sheet (not shown) as a site whose albedo is expected to remain fairly constant over a long period
12 (Riihelä et al., 2013). The results showed that the maximum deviation of monthly mean CLARA-A2 SAL over
13 this site from its 34-year mean was 8.5 %, including some natural variability associated with e.g. varying SZA.
14 Also, the 34-year mean albedo for this site was estimated to be 0.786 which is somewhat lower than the literature
15 citations for the albedo of dry fresh snow (0.85, Konzelmann and Ohmura, 1995).

16 The cloud mask used in CLARA-A2 SAL is less conservative than the one used in CLARA-A1 SAL. This is
17 likely to affect the SAL values especially during non-continuous cloud conditions. Also the inaccuracies in the
18 land cover data record used to resolve the CLARA-A2 SAL algorithms may cause retrieval errors. The users are
19 recommended to utilize the existing support data (for example number of observations, standard deviation, mean
20 SZA, skewness and kurtosis per pixel) to remove suspect retrievals from their analysis.

21 Our quality assessment of the CLARA-A1 SAL surface albedo data record has shown that SAL retrievals over
22 snow and ice, particularly over the Arctic, are of good quality (Riihelä et al., 2010). Also, according to user
23 feedback, the data record has been useful for climate model validation (e.g., Light et al., 2015). The retrieval
24 over snow and ice is essentially the same in CLARA-A2 SAL as it was for the previous edition of the data
25 record which gives reason to believe that the user feedback and quality assessment should, to some extent, also
26 be valid for CLARA-A2. The validation results against in situ observations and comparison with MODIS
27 MCD43C3 product show that adding the new AOD time series for land areas has improved the algorithm
28 performance elsewhere as well.

29

30 **6 Surface radiation products**

31 The retrieval algorithms to derive the CLARA-A2 surface radiation products have only undergone minor
32 changes since CLARA-A1. Details on the algorithms are given in Karlsson et al., (2013). Thus, this section
33 presents a few validation results of the CLARA-A2 surface radiation data records.

34 **6.1 Surface Solar Irradiance**

35 The spatial data coverage of the surface solar irradiance (SIS) data has been substantially improved. In CLARA-
36 A2, only snow-covered surfaces are excluded due to a reduced accuracy of the SIS data under these conditions.

1 The validation against surface reference measurements from the Baseline Surface Radiation Network (BSRN)
2 documents the improved accuracy of the CLARA A2 surface irradiance data record, mainly due to the improved
3 cloud detection (see Table 32).

4 Figure 132 presents the comparison of the decadal linear trends derived from the CLARA-A2 SIS data record
5 with the corresponding trends derived from measurements obtained from the BSRN. To assess the validity of the
6 linear trend derived from the CLARA data record, only surface stations with continuous observations covering at
7 least 10 years of measurements are used.

8 The trends derived from the CLARA-A2 surface irradiance record correspond well to the trends derived from the
9 BSRN measurements, indicating the high stability of the satellite-derived product and its suitability to calculate
10 temporal changes and trends (Fig. 132). For most BSRN stations, the decadal trend is positive during the
11 considered time period. Note that the time period for which BSRN measurements are available differs between
12 the stations; consistent time periods were used to compare the CLARA-A2 SIS data record with the BSRN
13 measurements at each station.

14 Figure 143 presents the spatial distribution of the decadal linear trend between 1992 and 2015 based on the
15 CLARA-A2 SIS data record ~~in over~~ Europe and ~~parts a portion~~ of Northern America. To limit the impact of the
16 missing data during the first decade of the CLARA-A2 SIS data record due to the availability of only one
17 AVHRR instrument, the trend was derived starting in 1992, when at least two AVHRR instruments have been
18 available. In both regions there is an overall positive trend in surface irradiance, consistent with surface
19 observations (e.g., Wild, 2012).

20 6.2 Surface Longwave Radiation

21 The CM SAF CLARA-A2 data record provides information on the surface longwave downwelling (SDL) and
22 outgoing (SOL) radiation in order to enable studies of the full surface radiation budget. Both data records are
23 dependent upon the surface ~~and TOA~~ longwave radiation records from the ERA-Interim reanalysis (Dee et al.,
24 2009); using topographic information and the monthly mean cloud fraction from CLARA-A2, the ERA-Interim
25 data are downscaled to match the spatial resolution of the CLARA-A2 data record. For SOL, this means a pure
26 downscaling of ERA-Interim data. For SDL, an effective cloud factor is derived, based on ERA-Interim
27 differences in clear-sky and all-sky downwelling longwave radiation, and reanalysis cloud fraction (Karlsson et
28 al., 2013). This factor is then downscaled to CLARA-A2 resolution and multiplied by the CLARA-A2 satellite-
29 derived cloud fraction. The result is a hybrid estimate of combined satellite-reanalysis SDL.

30 Table 43 shows the validation results of the monthly mean CLARA-A2 SOL and SDL data records compared to
31 measurements obtained from the BSRN network. The improved cloud mask in CLARA-A2 led to a substantial
32 improvement of the data quality of SDL data record relative to the CLARA-A1 data record.

34 7 Discussion: Demonstration of potential applications

35 The improvements of the underlying AVHRR radiance data record, the upgraded retrieval methods and the 6-
36 year prolongation of the observation time series all increase the usefulness of the CLARA CDR for many

1 applications. In other words, the potential for the data record to quantify true climate variability and trends has
2 improved.

3 In this section, ~~we provide two examples demonstrating we wish to provide some exploratory results that can be~~
4 ~~directly derived from different applications of the new CLARA-A2 CDR, highlighting the potential value for~~
5 ~~different applications and future research directions. The demonstrated results should be viewed as preliminary~~
6 ~~results requiring further detailed analysis. The purpose of presenting them here is meant to encourage in depth~~
7 ~~follow on studies.~~

8 The first example ~~deals-consider~~ with the following question: How have surface and cloud conditions changed
9 in the Arctic region ~~during-over~~ the last three to four decades? Similar studies on Arctic surface albedo variations
10 alone have already been made based on CLARA-A1 data (Riihelä et al., 2013), but access to a longer time series
11 of observations (including the new record year 2012 in Arctic minimum sea ice extent) and the coupling to cloud
12 processes clearly motivate continued studies in this field. Many climate predictions and scenarios point ~~at~~
13 ~~towards~~ the existence of an Arctic amplification (e.g., Cohen et al., 2014) of the ~~regional~~ temperature rise due to
14 several large positive feedback effects; two of these effects are the decrease of sea ice cover and its interaction
15 with cloud~~iness-cover~~. The good AVHRR observation conditions during the polar summer season (e.g., as
16 pointed out in ~~S~~section 3.1 discussing Fig. ~~ure 54~~) now permit more in depth studies of these two aspects.

17 Figure ~~154~~ shows the mean change of SAL for the first decade of the CLARA-A2 period (1982-1991) compared
18 to the last decade (2006-2015) over the high-latitude Northern Hemisphere ~~during-the~~ summer months. The
19 corresponding changes in mean cloud cover are shown in Fig. ~~165~~. We can clearly see the strong SAL signal
20 associated with Arctic sea ice decline since the 1980s, which is very evident in all months from May through
21 September. Corresponding changes in Arctic cloudiness (Fig. ~~165~~) ~~appear-are, however,~~ not as equally
22 systematic and well depicted. This is not surprising since cloud conditions depend primarily on atmospheric
23 circulation patterns. However, we notice a tendency for increased cloud cover over the marginal ice zone and the
24 new ice-free regions of the inner Arctic in the months July-September while some decreases in cloud cover can
25 be seen over the remaining ice-covered parts (e.g. close to Greenland and the Canadian archipelago). This result,
26 based on long-term CLARA-A2 data, supports the findings by Devasthale et al. (2016) regarding a similar co-
27 variability between cloudiness and sea-ice concentration observed in the last decade. An interesting feature in
28 April-May is also the increase in cloud cover in the inner Arctic region while cloudiness appears to decrease
29 outside of this area. ~~However, f~~urther studies ~~should-are needed to~~ investigate the significance of these patterns
30 and the possible links to changes in circulation and radiation conditions. For these purposes, the entire CLARA-
31 A2 data record (i.e., including years 1992-2005) must be used.

32 Another ~~application-example~~ is related to studies of cloud-climate feedback processes which are known to
33 explain a large part of the uncertainty in climate scenarios from ~~climate-model~~ ~~simulations~~s. Norris et al. (2016)
34 claim that we can already now see changes in global cloud patterns from long-term satellite observations, which
35 are supported by climate model simulations. Specifically, the authors claim that there are signs of a decrease in
36 mid-latitude cloudiness indicating “a poleward expansion of the subtropical dry zone cloud minimum and a
37 poleward retreat of the storm-track cloud maximum”, based on a combined analysis of data from the ISCCP
38 (Rossow and Schiffer, 1999) and PATMOS-x (Heidinger et al., 2104) climate data records covering the period

1 1983-2009. Similar changes in cloud patterns have been noticed in corresponding CMIP5 historical simulations
2 (Norris et al., 2016).

3 Since CLARA-A2 is based on the same basic satellite radiance data record as PATMOS-x, and only differing in
4 cloud retrieval methods, we could potentially see the same cloud changes. The CLARA-A2 availability of results
5 for an additional 7 year period (with more stable satellite data less impacted by e.g., orbital drift effects) should
6 also help giving some indication if the reported cloud change features remain or if they have changed in some
7 way. Figure 176 shows the linear trend (note color scale is inverted relative to traditional depictions, where cold
8 (warm) colors indicated positive (negative) cloud fraction trends), expressed as cloud fraction change over a 25-
9 year period but now estimated from 34 years of CLARA-A2 data, in comparison to only 27 years of data
10 analysed by Norris et al. (2016). Comparisons with corresponding results by Norris et al. (2016) reveal many
11 similarities, especially in the changed cloud distribution at low and tropical latitudes. It is apparent that in the
12 latter part of the 34-year period we have had some dominance of strong El Nino events (e.g. 1997-1998 and
13 2015-2016) explaining the typical El Nino pattern over the central Pacific and Indonesia/Australia regions in Fig.
14 176. Interestingly, this signal is not as strong as in the study by Norris et al. (2016) which shows the value of
15 studying a longer period where the ENSO extremes have a better chance of neutralizing each other in the long-
16 term mean.

17 We notice that ~~changes in~~ cloud distribution changes in other regions (e.g. the positive trends over Africa and in
18 the eastern Pacific region) cannot be as clearly linked to typical El Nino Southern Oscillation (ENSO) patterns
19 which is interesting. Whereas the agreement with Norris et al., (2016) is very good at low and tropical latitudes,
20 the changes seen at mid- and high latitudes in the CLARA-A2 results are not as conclusive. There are some
21 dominant negative trends over the typical extra-tropical storm track regions over the northern parts of the
22 Atlantic and Pacific oceans but a similar change over the southern oceanic regions is not evident. We also see
23 discrepancies over the eastern part of the Eurasian continent where CLARA-A2 shows a dominant decreasing
24 trend. Based on these results we find it difficult to conclusively support the suggestions by Norris et al. (2016)
25 regarding cloud changes at mid- and high-latitudes. If we consider the cloud trends derived from PATMOS-x
26 and ISCCP separately (conclusions were drawn from a composited ISCCP-PATMOS-x data record), which were
27 also provided by Norris et al. (2016), we find that mid-latitude trends for PATMOS-x show a better agreement
28 with CLARA-A2 trends. This highlights the strength of data records comprised from polar-orbiting satellites,
29 where better coverage of mid- and high-latitude regions is possible. Further studies are needed here to
30 understand these differences.

31 A final remark regarding the use of CLARA-A2 results in climate model evaluation studies is that a COSP cloud
32 observation simulator (Bodas-Salcedo et al., 2011) for CLARA-A2 is under preparation for facilitating
33 comparisons with satellite-based results. In that way artefacts in the satellite observation and adequate
34 corrections for viewing and observation conditions can be applied in order to give a more realistic inter-
35 comparison of results between models and CLARA-A2 cloud products.

36

1 **8 Summary and future plans**

2 We have described the CLARA-A2 dataset – an improved 34-year cloud, surface albedo and radiation budget
3 data record based on data from the AVHRR sensor on polar orbiting operational meteorological satellites. Major
4 improvements in both the underlying AVHRR radiances and in the retrieval schemes have been described,
5 together with some validation results. Regarding the latter, we have selected a limited glimpse at the exhaustive
6 results created through the extensive validation efforts that have been conducted. More results and analyses are
7 planned in follow-on papers. Some typical applications have also been demonstrated to encourage such studies
8 using CLARA-A2 data records. We would also like to highlight the broadening of the CLARA portfolio of
9 products which now also include daily aggregated and resampled orbits (level 2b) and the existence of an
10 experimental data record on probabilistic cloud masks. Related to this is ~~also~~ the development of a CLARA-A2
11 cloud dataset COSP simulator.

12 A continuation of this work has recently been secured by the EUMETSAT approval of the third continuous
13 operations and development phase (CDOP-3) of the CM SAF project covering the years 2017-2022. This means
14 that a third edition of CLARA (CLARA-A3) is planned for release by the end of the CDOP-3 phase. This would
15 be the last edition based entirely on original AVHRR data, including data from METOP-C (the last polar satellite
16 carrying the AVHRR instrument). Furthermore, it will include an extension of the dataset with data forward in
17 time for the years 2016-2020 and backward in time to 1978 (including data from the AVHRR/1 sensor starting
18 with the Tiros-N satellite), which means it will cover more than 40 years in time. The product dataset will then
19 also be extended with top of atmosphere radiation products and the original AVHRR radiances (level 1) will take
20 advantage of a revised infrared calibration (following Mittaz and Harris, 2009), in addition to the upgraded
21 visible calibration.
22

1 **Appendix A: Acronym list**

2	AOD	Aerosol Optical Depth
3	ATBD	Algorithm Theoretical Basis Document
4	AVHRR	Advanced Very High Resolution Radiometer (NOAA)
5	BSRN	Baseline Surface Radiation Network
6	CALIOP	Cloud-Aerosol Lidar with Orthogonal Polarisation (CALIPSO)
7	CALIPSO	Cloud-Aerosol Lidar and Infrared Pathfinder Satellite Observation
8		satellite (NASA)
9	CDR	Climate Data Record
10	CERES	Clouds and the Earth's Radiant Energy System (NASA)
11	CFC	Cloud Fractional Cover product
12	CFMIP	Cloud Feedback Model Intercomparison Project
13	CLARA-A	The CM SAF cLoud, Albedo and surface RAdition dataset from
14		AVHRR data
15	CM SAF	Climate Monitoring Satellite Application Facility (EUMETSAT)
16	COSP	CFMIP Observation Simulation Package
17	COT	Cloud Optical Thickness product
18	CPH	Cloud Phase product
19	CPP	Cloud Physical Products package
20	CTO	Cloud TOp level product
21	DAK	Doubling-Adding KNMI radiative transfer model
22	ECMWF	European Centre for Medium-range Weather Forecasts
23	ENSO	El Nino Southern Oscillation
24	ERA-Interim	ECMWF ReAnalysis Interim dataset
25	EUMETSAT	EUropean organisation for exploitation of METeorological
26		SATellites
27	FCDR	Fundamental Climate Data Record
28	GAC	Global Area Coverage (AVHRR, 5 km global resolution)
29	GCOS	Global Climate Observing System (WMO)
30	GEWEX	Global Energy and Water cycle EXperiment

1	ISCCP	International Satellite Cloud Climatology Project
2	ITCZ	Inter-Tropical Convergence Zone
3	IWP	Ice Water Path product
4	JCH	Joint Cloud property Histograms
5	LUC	Land Use Classification
6	LUT	Look Up Table
7	LWP	Liquid Water Path product
8	MCD43C3	MODerate-resolution Imaging Spectroradiometer (MODIS) Albedo product
9	MODIS	Moderate Resolution Imaging Spectroradiometer (NASA)
10	NASA	National Aeronautics and Space Administration (USA)
11	NOAA	National Oceanographic and Atmospheric Administration (USA)
12	NWCSAF	Nowcasting Satellite Application Facility (EUMETSAT)
13	PATMOS-x	The AVHRR Pathfinder Atmospheres Extended dataset (NOAA)
14	PPS	Polar Platform Systems package (EUMETSAT, NWCSAF)
15	PUM	Product User Manual
16	PyGAC	Python module for AVHRR GAC pre-processing
17	REFE	Cloud Effective Radius product
18	RTM	Radiative Transfer Model
19	SAL	Surface ALbedo product
20	SMMR	Scanning Multichannel Microwave Radiometer (Nimbus 7 satellite)
21	SSM/I	Special Sensor Microwave Imager
22		(Defense Meteorological Satellite Program – DMSP – satellites)
23	SYNOP	Synoptical weather observations from surface stations
24	TOA	Top Of Atmosphere
25	VAL	VALidation report
26	WCRP	World Climate Research Programme
27	WMO	World Meteorological Organisation
28		
29		
30		

1 **Acknowledgements**

2 The authors want to thank Dr. Andrew Heidinger at NOAA for providing the method for inter-calibrating
3 historic visible AVHRR radiances.

4 This work is funded by EUMETSAT in cooperation with the national meteorological institutes of Germany,
5 Sweden, Finland, the Netherlands, Belgium, Switzerland and United Kingdom.

6 The CLARA-A2 data record is (as all CM SAF CDRs) freely available via the website <https://www.cmsaf.eu>.

7

1 **References**

- 2 Bodas-Salcedo, A., Webb, M.J., Bony, S., Chepfer, H., Dufresne, J.-L., Klein, S.A., Zhang, Y., Marchand, R.,
3 Haynes, J.M., Pincus, R. and John, V.O.: COSP: Satellite simulation software for model assessment, *Bull. Amer.*
4 *Meteor. Soc.*, August 2011, 1023-1043, doi: 10.1175/2011BAMS2856.1 , 2011.
- 5 Cohen, J., Screen, J.A., Furtado, J.C., Barlow, M., Whittleston, D., Coumou, D., Francis, J., Dethloff, K.,
6 Entekhabi, D., Overland, J. and Jones, J.: Recent Arctic amplification and extreme mid-latitude weather. *Nature*
7 *Geoscience*, 7, 627-637, doi:10.1038/ngeo2234, 2014.
- 8 Dee, D. P., Uppala, S. M., Simmons, A. J., Berrisford, P., Poli, P., Kobayashi, S., Andrae, U., Balmaseda, M. A.,
9 Balsamo, G., Bauer, P., Bechtold, P., Beljaars, A. C. M., van de Berg, L., Bidlot, J., Bormann, N., Delsol, C.,
10 Dragani, R., Fuentes, M., Geer, A. J., Haimberger, L., Healy, S. B., Hersbach, H., Hólm, E. V., Isaksen, L.,
11 Källberg, P., Köhler, M., Matricardi, M., McNally, A. P., Monge-Sanz, B. M., Morcrette, J.-J., Park, B.-K.,
12 Peubey, C., de Rosnay, P., Tavolato, C., Thépaut, J.-N., Vitart, F.: The ERA-Interim reanalysis: configuration
13 and performance of the data assimilation system, *Quarterly Journal of the Royal Meteorological Society*, 137,
14 656, (doi = 10.1002/qj.828), 553—597, 2011.
- 15 De Haan, J. F., Bosma, P. and Hovenier, J.W.: The adding method for multiple scattering calculations of
16 polarized light, *Astron. Astrophys.*, 183, 371-391, 1987.
- 17 Delanoë, J., and R. J. Hogan: A variational scheme for retrieving ice cloud properties from combined radar,
18 lidar, and infrared radiometer, *J. Geophys. Res.*, 113, D07204, doi:10.1029/2007JD009000, 2008.
- 19 Derrien, M. and LeGleau, H.: Improvement of cloud detection near sunrise and sunset by temporal-differencing
20 and region-growing techniques with real-time SEVIRI, *Int. J. Remote Sens.*, 31, 1765-1780,
21 DOI:10.1080/01431160902926632, 2010.
- 22 Devasthale, A., J. Sedlar, B. Kahn, M. Tjernström, E. Fetzer, B. Tian, J. Teixeira, and T. Pagano: A decade of
23 space borne observations of the Arctic atmosphere: novel insights from NASA's Atmospheric Infrared Sounder
24 (AIRS) instrument. *Bull. Amer. Meteor. Soc.* doi:10.1175/BAMS-D-14-00202.1, 2016 (in press).
25 <http://journals.ametsoc.org/doi/pdf/10.1175/BAMS-D-14-00202.1>
- 26 Devasthale, A., Raspaud, M., Schlundt, C., Hanschmann, T., Finkensieper, S., Dybbroe, A., Hörnquist, S.,
27 Håkansson, N., Stengel, M. and Karlsson, K.-G.: PyGAC: an open-source, community-driven Python interface
28 to preprocess more than 30-year AVHRR Global Area Coverage (GAC) data. 2016 (in preparation).
- 29 Dybbroe, A., Thoss, A. and Karlsson, K.-G.: NWCSAF AVHRR cloud detection and analysis using dynamic
30 thresholds and radiative transfer modelling – Part I: Algorithm description, *J. Appl. Meteor*, 44, 39-54, 2005.
- 31 Eastwood, S.: Sea Ice Product User's Manual OSI-401-a, OSI-402-a, OSI-403-a. Version 3.11. September 2014,
32 http://osisaf.met.no/docs/osisaf_ss2_pum_ice-conc-edge-type.pdf, doi: 10.15770/EUM_SAF_OSI_0005
33 (https://www.researchgate.net/publication/294892033_OSI_SAF_global_sea_ice_concentration_data_record_-_OSI-409a)
34

1 Gascard, J.-C., Bruemmer, B., Offermann, M., Doble, M., Wadhams, P., Forsberg, R., Hanson, S., Skourup, H.,
2 Gerland, S., Nicolaus, M., Metaxian, J.-P., Grangeon, J., Haapala, J., Rinne, E., Haas, C., Heygster, G.,
3 Jakobson, E., Palo, T., Wilkinson, J., Kaleschke, L., Claffey, K., Elder, B., and Bottenheim, J.: Exploring Arctic
4 Transpolar Drift During Dramatic Sea Ice Retreat, *EOS*, 89, 21–28, 2008.

5 Heidinger, A.K., Straka, W.C., Molling, C.C., Sullivan, J.T. and Wu, X.Q.: Deriving an inter-sensor consistent
6 calibration for the AVHRR solar reflectance data record. *Int. J. Rem. Sens.*, 31(24), 6493-6517, 2010.

7 Heidinger, A. K., Foster, M. J., Walther, A. & Zhao, Z.: The Pathfinder Atmospheres Extended (PATMOS-x)
8 AVHRR climate data set. *Bull. Am. Meteorol. Soc.* 95, 909–922, 2014.

9 Jääskeläinen, E., Manninen, T., Tamminen, J. and Laine, M.: An Aerosol Optical Depth time series 1982-2014
10 for atmospheric correction from OMI and TOMS Aerosol Index, *Atmospheric Measurement Techniques*
11 Discussion, doi:10.5194/amt-2016-180, 2016 (in preparation).

12 Karlsson K.-G. and A. Dybbroe: Evaluation of Arctic cloud products from the EUMETSAT Climate Monitoring
13 Satellite Application Facility based on CALIPSO-CALIOP observations. *Atmos. Chem. Phys.*, 10, 1789–1807,
14 2010.

15 Karlsson, K.-G. and E. Johansson: On the optimal method for evaluating cloud products from passive satellite
16 imagery using CALIPSO-CALIOP data: example investigating the CM SAF CLARA-A1 dataset. *Atmos. Meas.*
17 *Tech.*, 6, 1271–1286, www.atmos-meas-tech.net/6/1271/2013/ , doi:10.5194/amt-6-1271-2013, 2013.

18 Karlsson, K.-G., E. Johansson and A. Devasthale: Advancing the uncertainty characterisation of cloud masking
19 in passive satellite imagery: Probabilistic formulations for NOAA AVHRR data, *Rem. Sens. Env.* , 158, 126-
20 139; doi:10.1016/j.rse.2014.10.028, 2015.

21 Karlsson, K.-G., Riihelä, A., Müller, R., Meirink, J. F., Sedlar, J., Stengel, M., Lockhoff, M., Trentmann, J.,
22 Kaspar, F., Hollmann, R., and Wolters, E.: CLARA-A1: a cloud, albedo, and radiation dataset from 28 yr of
23 global AVHRR data, *Atmos. Chem. Phys.*, 13, 5351-5367, doi:10.5194/acp-13-5351-2013, 2013.

24 Konzelmann, T. and Ohmura, A.: Radiative fluxes and their impact on the energy balance of the Greenland Ice
25 Sheet, *Journal of Glaciology*, 41, 490–502, 1995.

26 Light, B., S. Dickinson, D. K. Perovich, and M. M. Holland: Evolution of summer Arctic sea ice albedo in
27 CCSM4 simulations: Episodic summer snowfall and frozen summers, *J. Geophys. Res. Ocean.*, 120(1), 1–20,
28 doi:10.1002/2014JC010149, 2015.

29 Mittaz, P.D. and Harris, R.: A Physical Method for the Calibration of the AVHRR/3 Thermal IR Channels 1:The
30 Prelaunch Calibration Data. *J. Atmos. Ocean. Tech.*, 26, 996-1019, doi: 10.1175/2008JTECHO636.1, 2009.

31 Nakajima, T., and M. D. King: Determination of the Optical Thickness and Effective Particle Radius of Clouds
32 from Reflected Solar Radiation Measurements. Part 1: Theory. *J. Atmos. Sci.* , 47, 1878-1893, 1990.

33 [Norris, J. R., R. J. Allen, A. T. Evan, M. D. Zelinka, C. W. O'Dell & Stephen A. Klein: Evidence for climate](#)
34 [change in the satellite cloud record, *Nature* 536, 72–75 \(04 August 2016\), doi:10.1038/nature18273, 2016.](#)

- Formaterat: Engelska (USA)
- Formaterat: Engelska (USA)
- Formaterat: Engelska (USA)
- Formaterat: Engelska (USA)
- Formaterat: Engelska (USA)

1 O'Dell, C.W., Wentz, F.J. and Bennartz, R.: Cloud Liquid Water Path from Satellite-Based Passive Microwave
2 Observations: A New Climatology over the Global Oceans. *J. Climate*, 21, 1721–1739,
3 doi:10.1175/2007JCLI1958.1, 2008.

4 [OSI SAF: The EUMETSAT OSI SAF Sea Ice Concentration Algorithm. Algorithm Theoretical Basis](#)
5 [Document, SAF/OSI/CDOP/DMI/SCI/MA/189, Version 1.5, 2016.](#)

6 Ohmura, A., Gilgen, H., Hegner, H., Müller, G., Wild, M., Dutton, E. G., Forgan, B., Fröhlich, C., Philipona, R.,
7 Heimo, A., König-Langlo, G., McArthur, B., Pinker, R., Whitlock, C. H., and Dehne, K.: Baseline Surface
8 Radiation Network (BSRN/WCRP): New Precision Radiometry for Climate Research., *Bulletin of the American*
9 *Meteorological Society*, 79, 2115–2136, doi:10.1175/1520-0477(1998)079h2115:BSRNBWi2.0.CO;2, 1998.

10 Pavolonis, M. J., Heidinger, A. K., and Uttal, T.: Daytime global cloud typing from AVHRR and VIIRS:
11 Algorithm description, validation, and comparison, *J. Appl. Meteorol.*, 44, 804-826, doi:10.1175/JAM2236.1,
12 2005.

13 Peltoniemi, J.I.; Kaasalainen, S.; Naranen, J.; Matikainen, L.; Piironen, J.: Measurement of directional and
14 spectral signatures of light reflectance by snow. *IEEE Transactions on Geoscience and Remote Sensing*, 43 (10),
15 2294- 2304, 2005.

16 Riihelä A., Laine V., Manninen T., Palo T., Vihma T.: Validation of the CM SAF surface broadband albedo
17 product: Comparisons with in situ observations over Greenland and the ice-covered Arctic Ocean. *Remote*
18 *Sensing of Environment*, 114 (11), 2779-2790, 2010.

19 Riihelä, A., Manninen, T. and Laine, V.: Observed changes in the albedo of the Arctic sea-ice zone for the
20 period 1982-2009, *Nature Climate Change*, 3, 895-898, doi:10.1038/nclimate1963, 2013.

21 Riihelä, A., Manninen, T., Laine, V., Andersson, K., and Kaspar, F.: CLARA-SAL: a global 28-yr timeseries of
22 Earth's black-sky surface albedo, *Atmos. Chem. Phys.* , 13, 3743-3762, doi:10.5194/acp-13-3743-2013, 2013.

23 Roebeling, R. A., A. J. Feijt, A.J. and Stammes, P.: Cloud property retrievals for climate monitoring:
24 implications of differences between SEVIRI on METEOSAT-8 and AVHRR on NOAA-17, *J. Geophys. Res.*,
25 111, D20210, doi:10.1029/2005JD006990, 2006.

26 Rossow, W. B. and Schiffer, R. A.: ISCCP Cloud Data Products. *Bull. Am. Meteorol. Soc.* 72, 2-20, doi:
27 10.1175/1520-0477(1991)072<0002:ICDP>2.0.CO;2, 1991.

28 Rossow, W. B. and Schiffer, R. A.: Advances in understanding clouds from ISCCP. *Bull. Am. Meteorol. Soc.*
29 80, 2261–2287, 1999.

30 [Sanchez-Lorenzo, A., A. Enriquez-Alonso, J. Calbó, J.-A. González, M. Wild, D. Folini, J. R. Norris and S. M.](#)
31 [Vicente-Serrano: Fewer clouds in the Mediterranean: consistency of observations and climate simulations.](#)
32 [Nature Scientific Reports 7, doi:10.1038/srep41475, 2017.](#)

33 Schaaf, C.B., Gao, F., Strahler, A.H., Lucht, W., Lia,X., Tsang, T., Strugnell, N.C., Zhang, X., Jin, Y., Muller,
34 J.-P., Lewis, P., Barnsley, M., Hobson, P., Disney, M., Roberts, G., Dunderdale, M., Doll, C., d'Entremont, R.P.,

1 Hu, B., Liang, S., Privette, J.L. and Royh, D.: First operational BRDF, albedo nadir reflectance products from
2 MODIS, *Remote Sens. Environ.*, 83, 2002.

3 Schulz, J., Albert, P., Behr, H.-D., Caprion, D., Deneke, H., Dewitte, S., Dürr, B., Fuchs, P., Gratzki, A.,
4 Hechler, P., Hollmann, R., Johnston, S., Karlsson, K.-G., Manninen, T., Müller, R., Reuter, M., Riihelä, A.,
5 Roebeling, R., Selbach, N., Tetzlaff, A., Thomas, W., Werscheck, M., Wolters, E., and Zelenka, A.: Operational
6 climate monitoring from space: the EUMETSAT Satellite Application Facility on Climate Monitoring (CM-
7 SAF), *Atmos. Chem. Phys.*, 9, 1687-1709, doi: 10.5194/acp-9-1687-2009, 2009.

8 Stammes, P.: Spectral radiance modelling in the UV-Visible range. IRS 2000: Current problems in Atmospheric
9 Radiation, edited by W.L. Smith and Y.M. Timofeyev, pp 385-388, A. Deepak Publ., Hampton, VA, 2001.

10 Stengel, M., A. Kniffka, J.F. Meirink, M. Lockhoff, J. Tan and R. Hollmann, CLAAS: the CM SAF cloud
11 property dataset using SEVIRI, *Atm. Chem. Phys.*, 14, 4297-4311, doi:10.5194/acp-14-4297-2014, 2014.

12 Stengel, M., S. Mieruch, M. Jerg, K.G. Karlsson, R. Scheirer, B. Maddux, J.F. Meirink, C. Poulsen, R. Siddans,
13 A. Walther and R. Hollmann, The Clouds Climate Change Initiative: Assessment of state-of-the-art cloud
14 property retrieval schemes applied to AVHRR heritage measurements, *Remote Sens. Environ.*,
15 doi:10.1016/j.rse.2013.10.035, 2013.

16 Stephens, G.: Radiation profiles in extended water clouds. II: Parameterization schemes. *J. Atmos. Sci.*, 35,
17 2123-2132, 1978.

18 Steffen, K., Box, J., and Abdalati, W.: Greenland Climate Network: GC-Net, CRREL 96-27 Special Report on
19 Glaciers, Ice Sheets and Volcanoes, tribute to M. Meier, pp. 98–103, 1996.

20 [Stevens, B., Vali, G., Comstock, K., Wood, R., van Zanten, M. C., Austin, P. H., Bretherton, C. S. and](#)
21 [Lenschow, D. H.: Pockets of open cells and drizzle in marina stratocumulus, *Bull. Amer. Met. Soc.*, January](#)
22 [2005, 51-57, 2005.](#)

23 [Sun, B., Free, M., Yoo, H. L., Foster, M. J., Heidinger, A. and Karlsson, K.-G.: Variability and Trends in US](#)
24 [Cloud Cover: ISCCP, PATMOS-x and CLARA-A1 Compared to Homogeneity-Adjusted Weather Observations,](#)
25 [J. Climate, June 2015. DOI: <http://dx.doi.org/10.1175/JCLI-D-14-00805.1>, 2015.](#)

26 Šuri, M., Huld, T.A., Dunlop, E.D. and Ossenbrink, H.A.: Potential of solar electricity generation in the
27 European Union member states and candidate countries. *Solar Energy*, 81, 1295-1305,
28 doi:10.1016/j.solener.2006.12.007, 2007.

29 Vaughan, M., Powell, K., Kuehn, R., Young, S., Winker, D., Hostetler, C., Hunt, W., Liu, Z., McGill, M., and
30 Getzewich, B.: Fully Automated Detection of Cloud and Aerosol Layers in the CALIPSO Lidar Measurements,
31 *J. Atmos. Oceanic Technol.*, 26, 2034–2050, doi: 10.1175/2009JTECHA1228.1, 2009.

32 Vial, J., Dufresne, J.-L. & Bony, S. On the interpretation of inter-model spread in CMIP5 climate sensitivity
33 estimates. *Clim. Dyn.* 41, 3339–3362, 2013.

34 Webb, M. J., Lambert, F. H. & Gregory, J. M. Origins of differences in climate sensitivity, forcing and feedback
35 in climate models. *Clim. Dyn.* 40, 677–707, 2013.

1 Wild, M.: Enlightening global dimming and brightening, Bull. Amer. Meteor. Soc., January 2012, 27-37,
2 <http://dx.doi.org/10.1175/BAMS-D-11-00074.1>, 2012.

3 Winker, D. M., Vaughan, M.A., Omar, A., Hu, Y, Powell, K.A., Liu, Z., Hunt, W.H., and Young, S.A.:
4 Overview of the CALIPSO mission and CALIOP data processing algorithms, J. Atmos. Oceanic. Technol., 26,
5 2310-2323, doi:10.1175/2009JTECHA1281.1, 2009.

6

7

1 **Table 1: CLARA-A2 level 3 cloud products.**

2

Product identifier	Product name	Description
CFC	Cloud Fractional Cover	Average fraction (%) of cloudy pixels in grid point.
CTO	Cloud Top level	Cloud top defined in one of three options: geometrical height (m), pressure (hPa) or brightness temperature (K).
CPH	Cloud phase	Average fraction (%) of liquid water cloud- pixels relative to all cloudy pixels. Product defined both day and night (new feature compared to CLARA-A1).
COT	Cloud Optical Thickness	Average (both linear and logarithmic) of cloud optical thickness for liquid and ice clouds separately (dimensionless).
REF	Cloud Effective Radius	Average of cloud particle sizes for liquid and ice clouds separately (μm).
LWP	Liquid Water Path	Average (in-cloud and all-sky) of column integrated liquid water (kgm^{-2}).
IWP	Ice Water Path	Average (in-cloud and all-sky) of column integrated frozen water (kgm^{-2}).
JCH	Joint Cloud Histogram	2-D histograms of occurrences in predefined cloud top pressure – cloud optical thickness bins. Defined for both water and ice clouds in a $1^\circ \times 1^\circ$ geographical grid. Only valid for daytime conditions (see text for further explanation).

3

4

5

6

7

8

9

10

1
2
3
4
5
6
7
8
9
10

Table 2: Globally averaged validation results of the CLARA-A2 and CLARA-A1 cloud detection (cloud mask) compared to CALIPSO-CALIOP observations based on 99 reference NOAA-18 and CALIPSO orbits in the period October 2006 to December 2009. Shown are the number of matched field of views (FOVs) and the validation scores mean error (bias), Kuipers and Hitrate.

<u>Data record</u>	<u># FOVs</u>	<u>Bias (%)</u>	<u>Kuipers</u>	<u>Hitrate (%)</u>
<u>CLARA-A2</u>	<u>787 102</u>	<u>-13.2</u>	<u>0.64</u>	<u>79.7</u>
<u>CLARA-A1</u>	<u>725 900</u>	<u>-14.4</u>	<u>0.56</u>	<u>75.8</u>

▲ -----
Formaterat: Teckensnitt:9 pt,
Teckenfärg: Svart, Engelska (USA)

1

2

3 | **Table 32:** Validation results of the CLARA-A2 surface irradiance (SIS) data record (monthly mean / daily
4 | mean) against the global data from the BSRN network; for reference the corresponding values for
5 | CLARA-A1 are also given. Shown are the number of months/days, the bias and the absolute bias as well
6 | as the correlation of the anomaly between the two CLARA data records and the BSRN data.

7

Data record	# obs	Bias (W/m²)	Abs. bias (W/m²)	Corr. Ano
CLARA-A2	6420 / 181649	-1.6 / -1.7	8.8 / 27.7	0.87 / 0.90
CLARA-A1	3105 / 96237	-3.3 / - 4.7	10.4 / 34.3	0.88 / 0.85

8

9

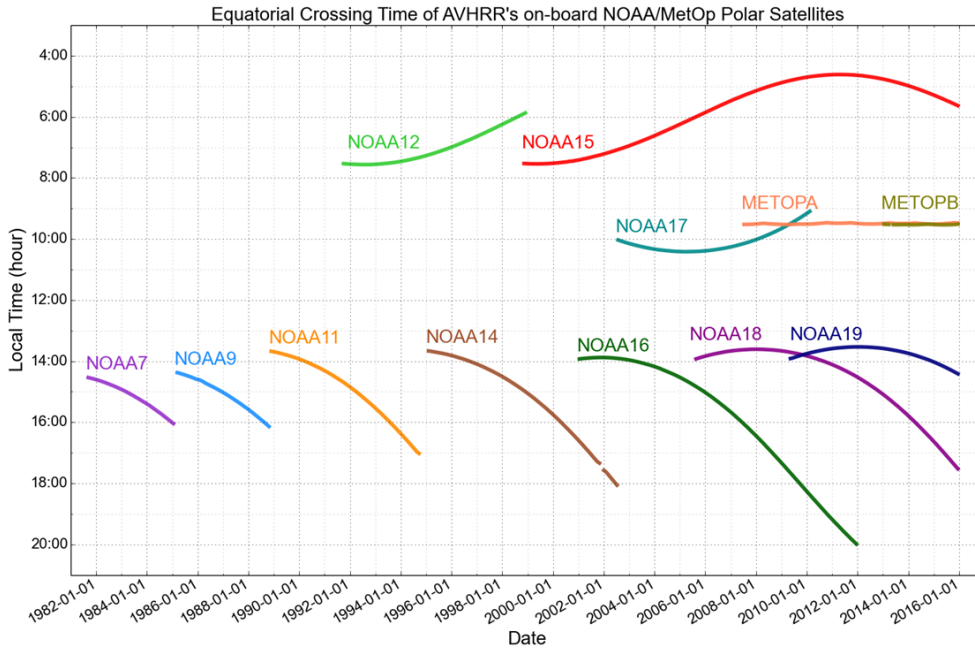
1
2
3
4
5
6
7
8

Table 43: Validation results of the monthly mean CLARA-A2 SOL and SDL data records compared to the measurements from the BSRN network. As references also the results obtained from CLARA-A1 and ERA-Interim are shown. Presented are the number of months used for the comparison, the bias and the absolute bias, as well as the correlation of the anomalies.

Data record	# Months	Bias (W/m ²)	Abs. bias (W/m ²)	Corr. Ano
SOL (A2/A1/ERA-I)	1680 / 1270 / 1680	2.9 / 5.8 / 1.9	13.7 / 13.8 / 14.1	0.74 / 0.71 / 0.78
SDL (A2/A1/ERA-I)	7302 / 5314 / 7302	-4.7 / -3.7 / -6.4	7.9 / 8.3 / 9.4	0.84 / 0.82 / 0.84

1

2



3

4 **Figure 1: Daytime equator observation times for all satellites covered by CLARA-A2 from NOAA-7 to**
5 **NOAA-19 and METOP A/B. The figure shows ascending (northbound) equator crossing times for all**
6 **afternoon satellites from NOAA-7 to NOAA-19 and descending (southbound) equator crossing times for all**
7 **morning satellites (NOAA-12, NOAA-15 NOAA-17 and METOP A+B). Corresponding night-time or**
8 **evening observations take place 12 hours earlier/later. Some data gaps are present but only for a number**
9 **of isolated dates.**

10

11

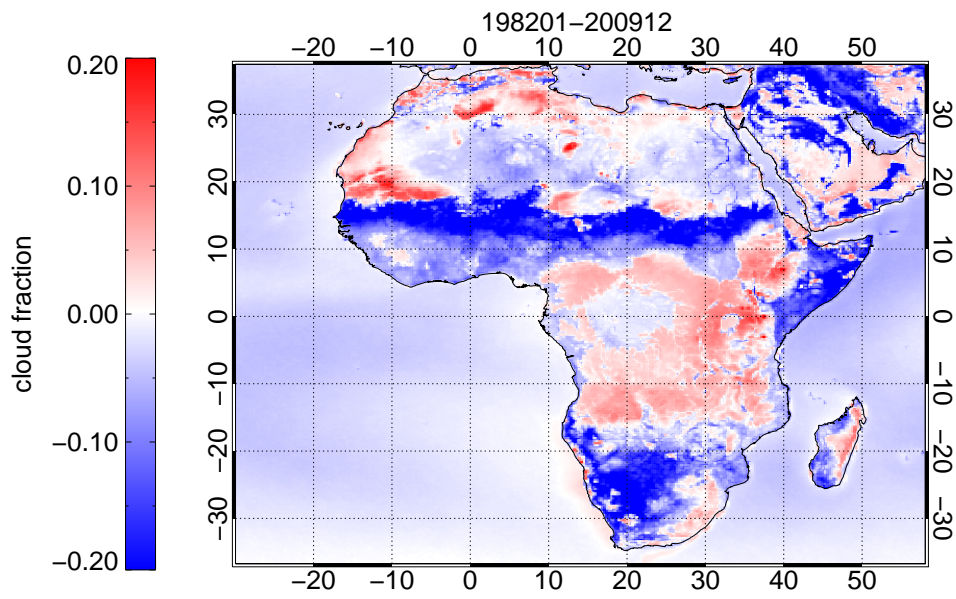
12

13

14

15 |

1



Formaterat: Centrerad

2

3

4

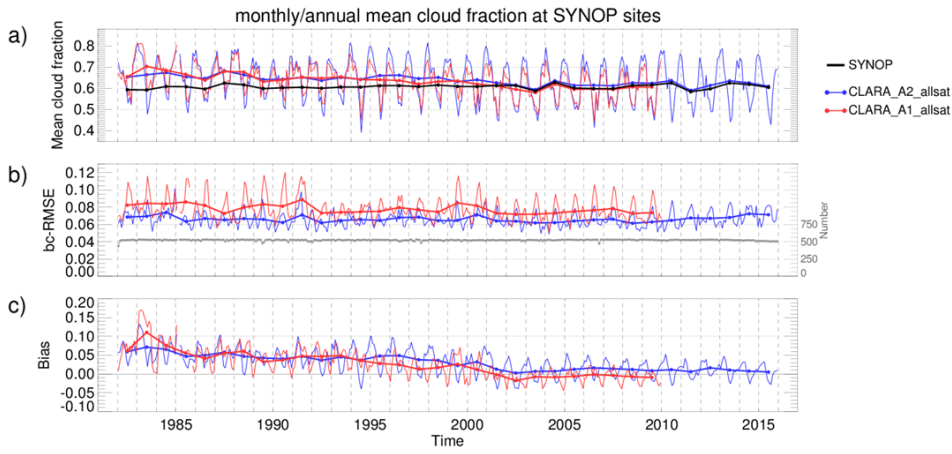
Figure 2: Mean difference in cloud fraction between CLARA-A2 and CLARA-A1 for the common period 1982-2009 over the African continent.

Formaterat: Beskrivning, Radavstånd: 1,5 rader

5

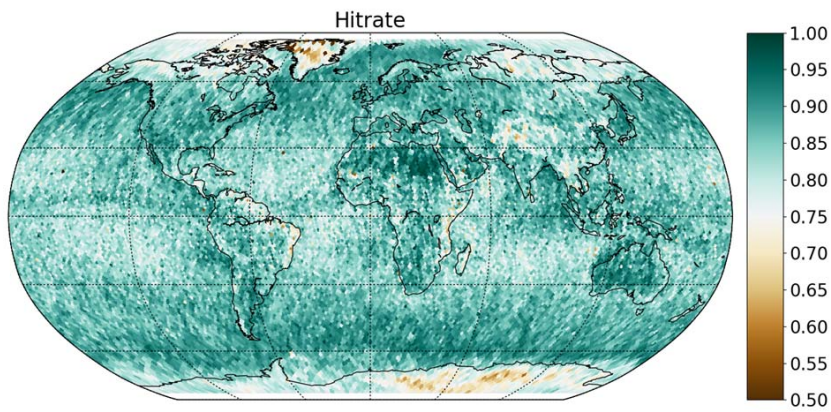
Formaterat: Teckensnitt:10 pt

1
2



3
4 | **Figure 32:** (a) Time series of mean monthly and annual cloud fraction for CLARA-A2 (blue), CLARA-A1
5 | (red), and SYNOP (black), (b) bias-corrected RMSE and (c) bias for the entire period 1982-2015. See text
6 | for further details.

1



2

3

4

5

6

7

8

9

10

11

Figure 43: Global overall frequency of correct cloudy and cloud-free estimations (often referred to as the Hitrate) derived from nearly 10 000 collocated (within 3 minutes) near-nadir AVHRR and CALIPSO-CALIOP orbits in the period 2006-2015. The Hitrate was calculated after discarding CALIOP-detected clouds with cloud optical thicknesses below 0.15. Results are collected in a Fibonacci grid with 28878 grid points evenly spread out around the Earth approximately 150 km apart. The resulting grid has almost equal area and almost equal shape of all grid cells. White spots are cells with insufficient coverage of collocations.

1
2
3
4
5
6
7
8
9

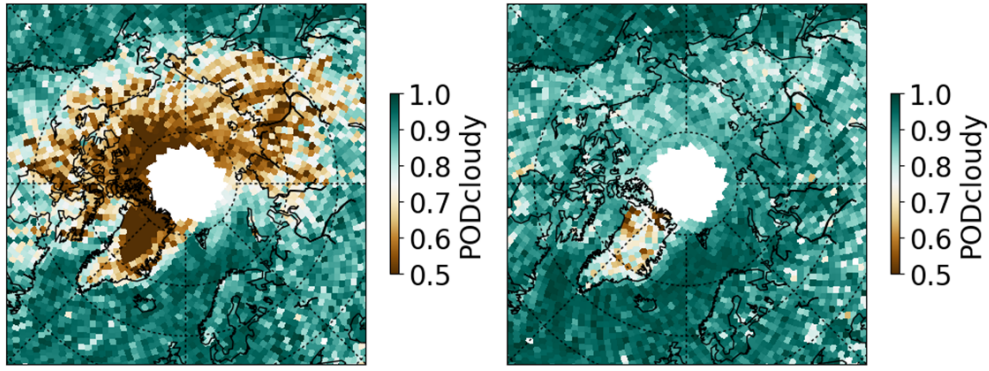
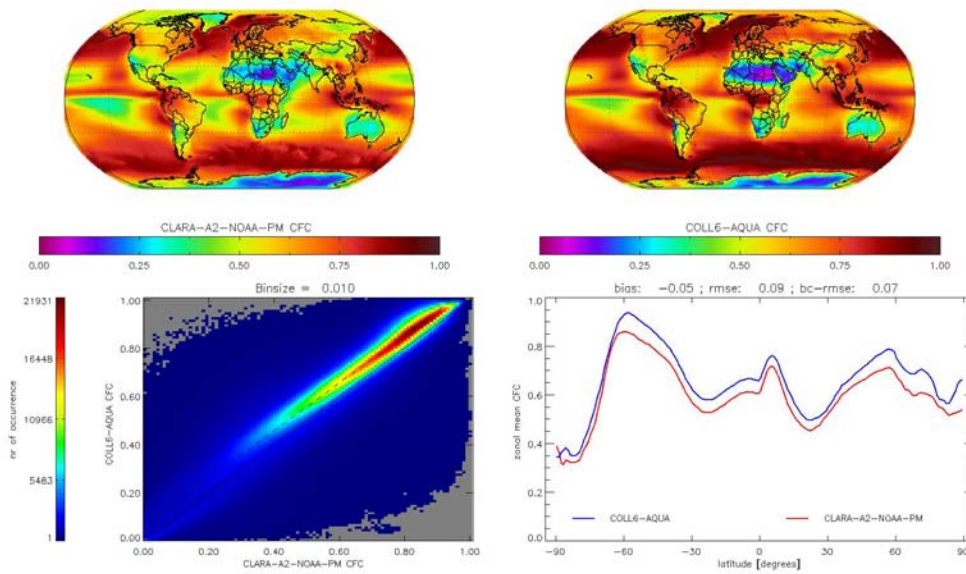


Figure 54: Probability of detecting cloudy conditions over the Arctic region during the pPolar wWinter (left) and during the pPolar sSummer (right). Results were derived from the same dataset as in Figure 3.

1

2



3

4

5

6

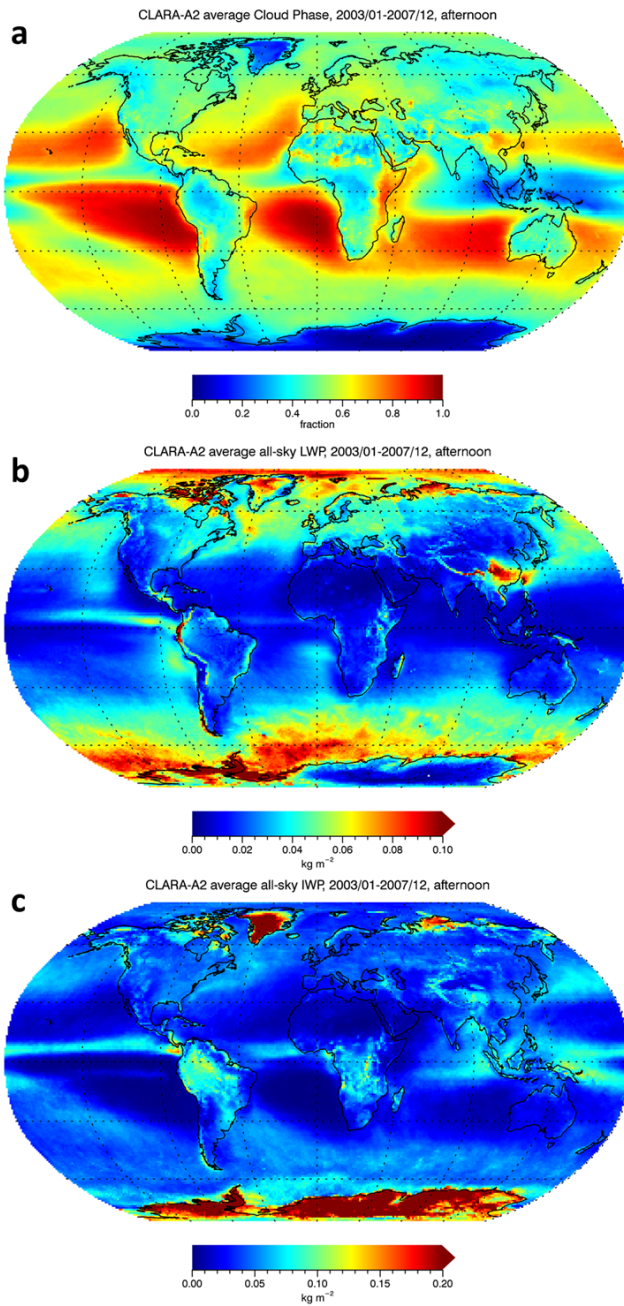
7

8

9

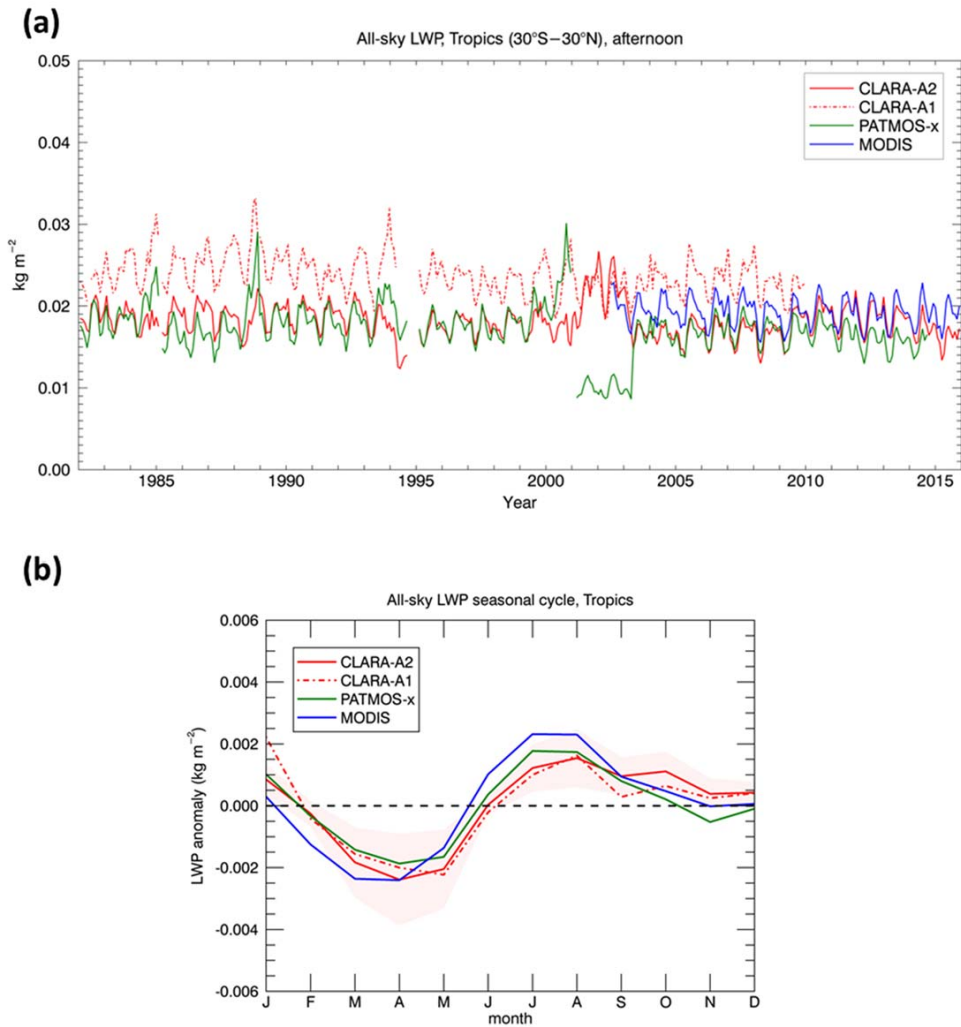
10

Figure 65: Intercomparison of CLARA-A2 and MODIS Collection 6 (Aqua part) cloud fraction over the covered MODIS period 2002-2014. Upper left: CLARA-A2 global cloud cover (CFC). Upper right: MODIS global cloud cover. Lower left: Scatterplot of the two data records. Lower right: Latitudinal distribution (zonal means) of cloud cover from the two data records (CLARA -A2 in red and MODIS in blue).



1
 2 | **Figure 76:** (a) Fraction of liquid clouds relative to total cloud fraction, (b) all-sky liquid water path and
 3 | (c) all-sky ice water path, averaged for the 5-year period 2003-2007. All data come from CLARA-A2 level
 4 | 3 products, derived from afternoon (NOAA-16 and NOAA-18) satellite measurements. Water paths in kg
 5 | m⁻².

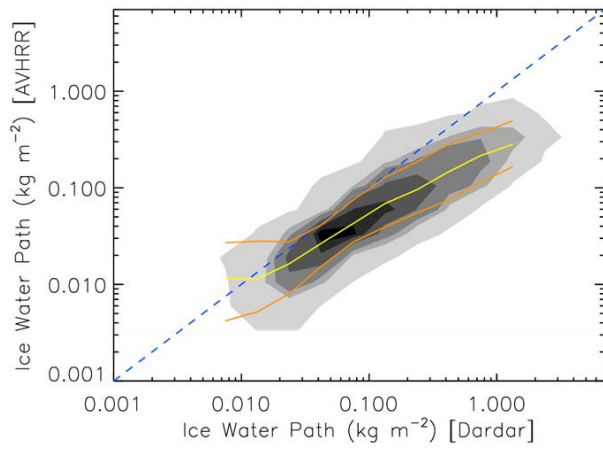
1



2

3 **Figure 87:** Comparison between CLARA-A2, CLARA-A1, PATMOS-x and MODIS all-sky liquid water
4 path (kgm^{-2}) for the Tropics (30S – 30N): monthly time series (top) and seasonal anomaly (bottom). The
5 seasonal anomaly is calculated as the average of the deviations of monthly means from the corresponding
6 yearly mean over the years 2003-200913. The shaded area around the CLARA-A2 curve indicates ± 1
7 standard deviation of these deviations. The plots have been compiled from the NOAA afternoon satellites
8 (NOAA-7, -9, -11, -14, -16, -18, and -19) for CLARA-A2, CLARA-A1 and PATMOS-x, and the MODIS
9 Aqua (MYD08 Collection 6) $3.7 \mu\text{m}$ product.

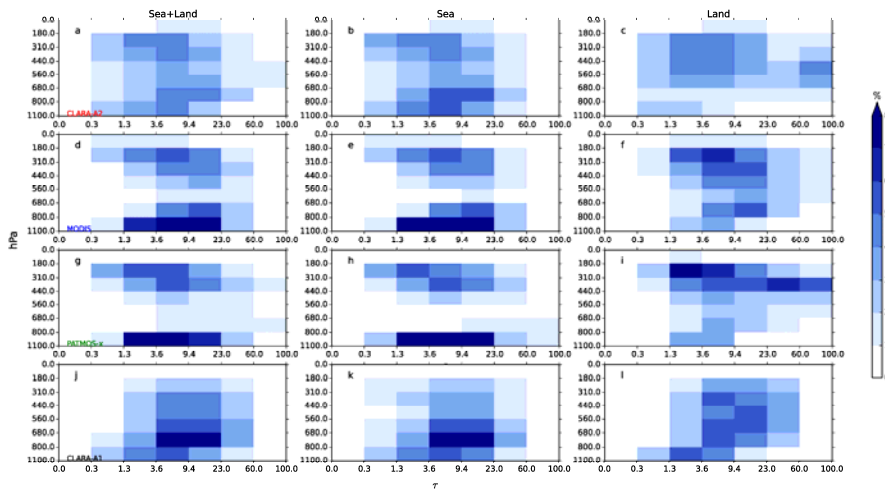
10



1
2
3
4
5
6
7

Figure 98: CLARA-A2 (NOAA-18) IWP vs. DARDAR IWP (kg m^{-2}) for the months January and July 2008. The yellow line depicts the median and orange lines the 16th/84th percentiles of the CLARA-A2 distribution at the corresponding DARDAR IWP. The greyscales indicate regions enclosing the 10, 20, 40, 60, and 75% of points with the highest occurrence frequency.

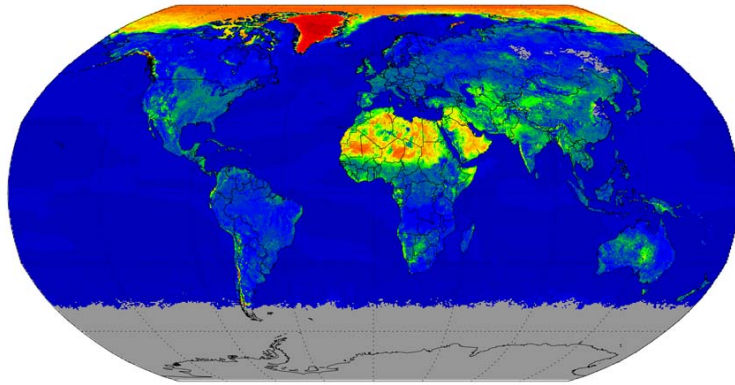
1
2
3
4



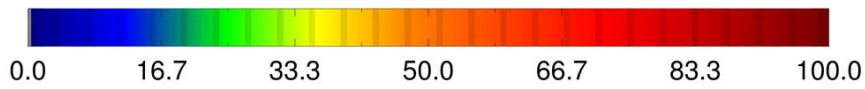
5
6
7
8
9
10
11
12
13
14
15

Figure 109: Global JCH relative frequency distributions [colors, %] of CTP [hPa] and COT for all months for four data records: CLARA-A2 (panels a-c), MODIS Collection 6 (panels d-f), PATMOS-X (panels g-i) and CLARA-A1 (panels j-l), during 2003-2014. The covered period is 2003-2013 except for CLARA-A1 which only covers the period 2003-2009 (no data after 2009). The top row (panels a-c) are CLARA-A2, the middle row (panels d-f) are MODIS Collection 6, and the bottom row (panels g-i) are for PATMOS-x. Left column contains the JCHs over sea and land surfaces (sea+land), middle column over sea-only surfaces (sea) and right column over land-only surfaces (land). Histogram frequencies are here normalized to unity, such that each histogram sums to 100%.

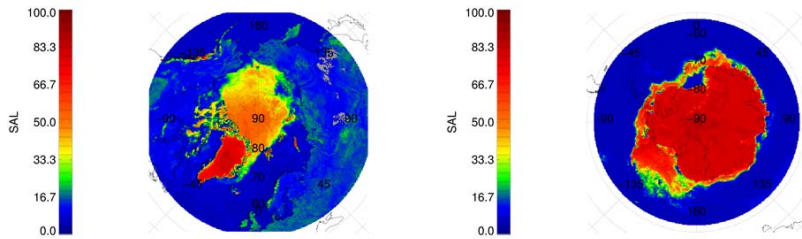
1
2
3
4



SAL



5



6

7

8

9

10

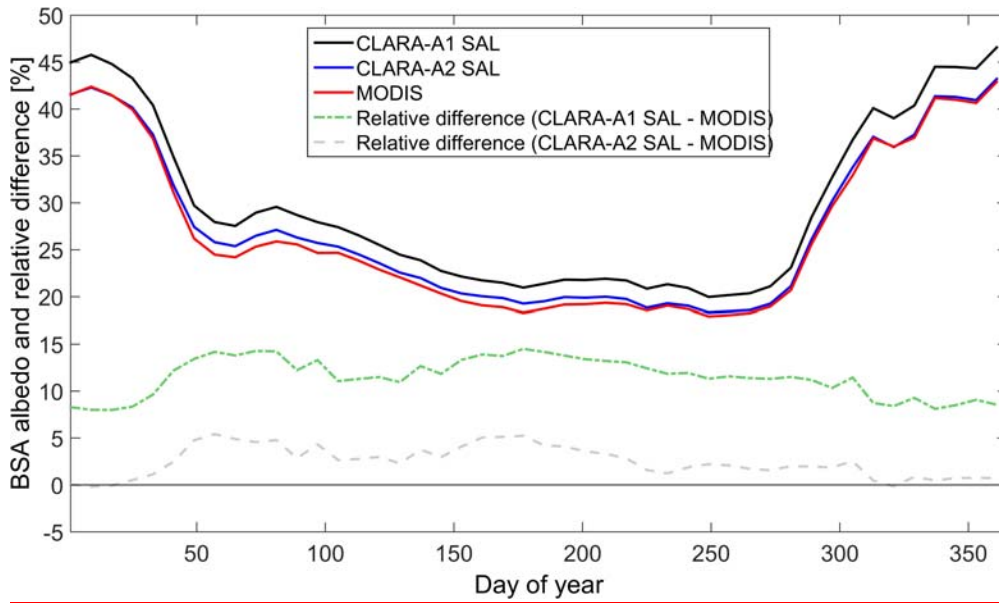
11

12

13

Figure 110: Global monthly mean surface albedo for July 2012 (top). Corresponding plots for two polar grids are shown at the bottom of the figure; one for the Arctic region (bottom left) and one for the Antarctic region (bottom right, but observe that the month here is January instead of July). Regions without values are grey-shaded (here resulting from dark conditions prevailing close to Antarctica during the pPolar winter). All albedos given as %.

1
2
3
4
5
6
7

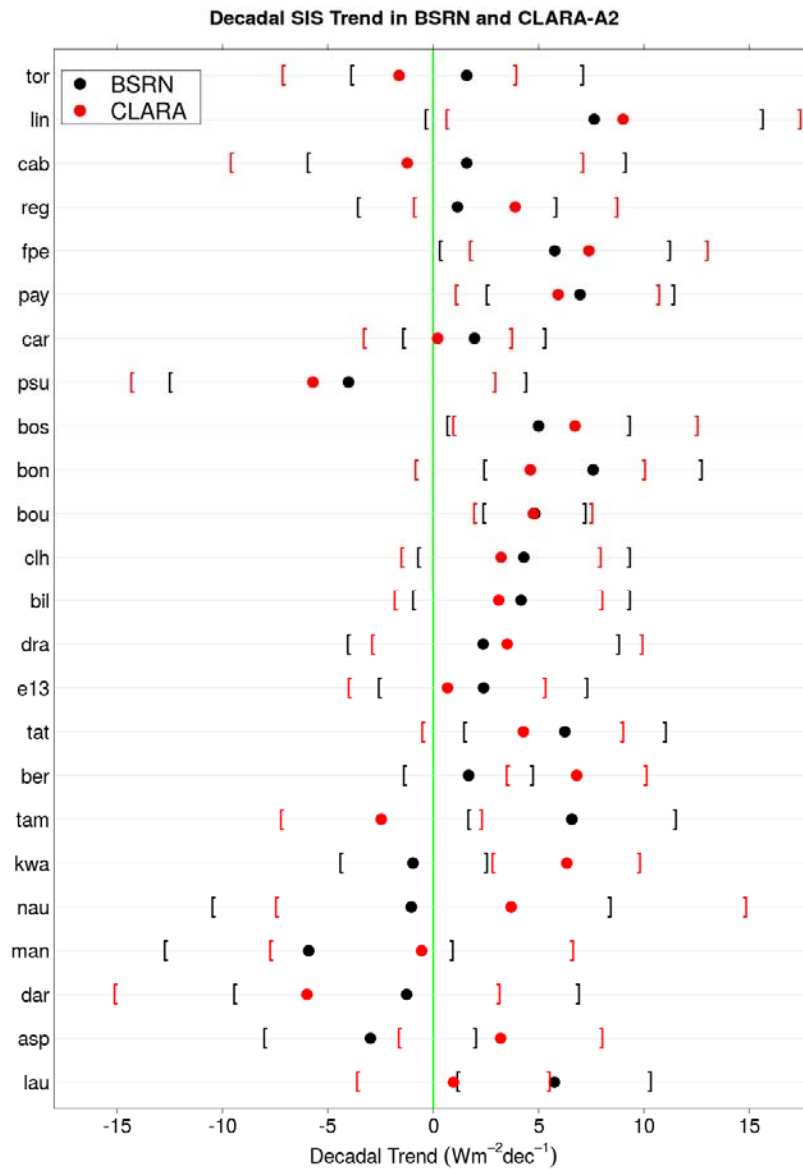


8
9

10 **Figure 124:** Comparison of surface albedos from CLARA-A2 SAL (blue line) and CLARA-A1 SAL
11 (black line) pentad composites with MODIS MCD43C3 (green-red line) results for 2009 [unit is per
12 cent]. The means are calculated only over those land/snow surfaces that are retrieved in both products,
13 the MODIS product is not defined for water bodies, thus they are excluded from this analysis. No
14 weighing for irradiance or area has been applied. The relative differences between the CLARA
15 products and MCD43C3 are products is shown with a grey (CLARA-A2) and green (CLARA-A1) dash-
16 dotted line.

17
18

1



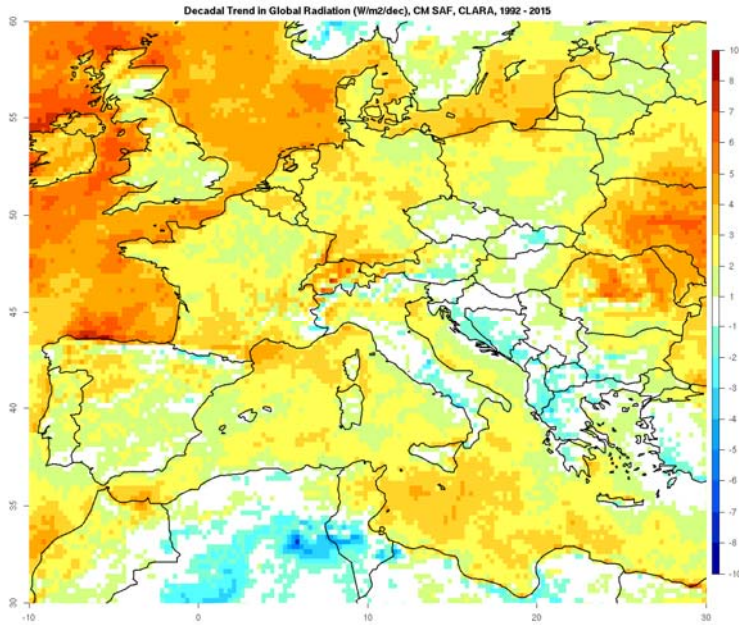
2
3 | Figure 132: Decadal linear trends derived from the CLARA-A2 surface irradiance data record (red dots)
4 | with the corresponding trends derived from measurements obtained from the BSRN (black dots).
5 | Trends are shown as $W_m^{-2}(\text{dec})^{-1}$. The parentheses represent the confidence interval of the trends. See
6 | text for further details.

7

1

2

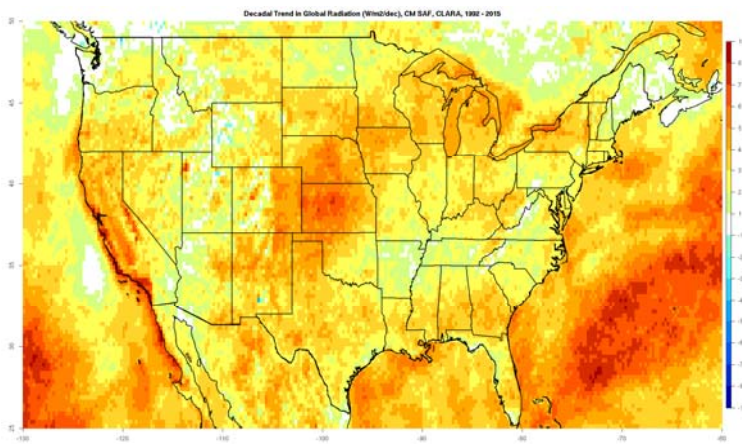
a)



3

4

b)



5

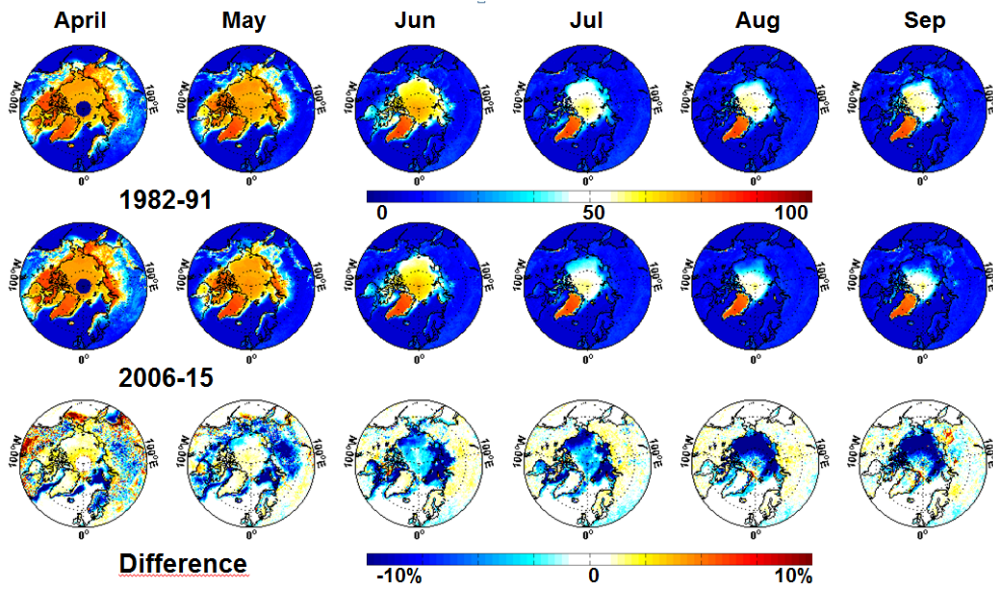
6

7

8

Figure 143: Decadal linear trend of the surface irradiance from 1992 to 2015 based on the CLARA-A2 SIS data record in (a) Central Europe and (b) parts of Northern America. All trends shown as $W \cdot m^{-2} \cdot (dec)^{-1}$.

1



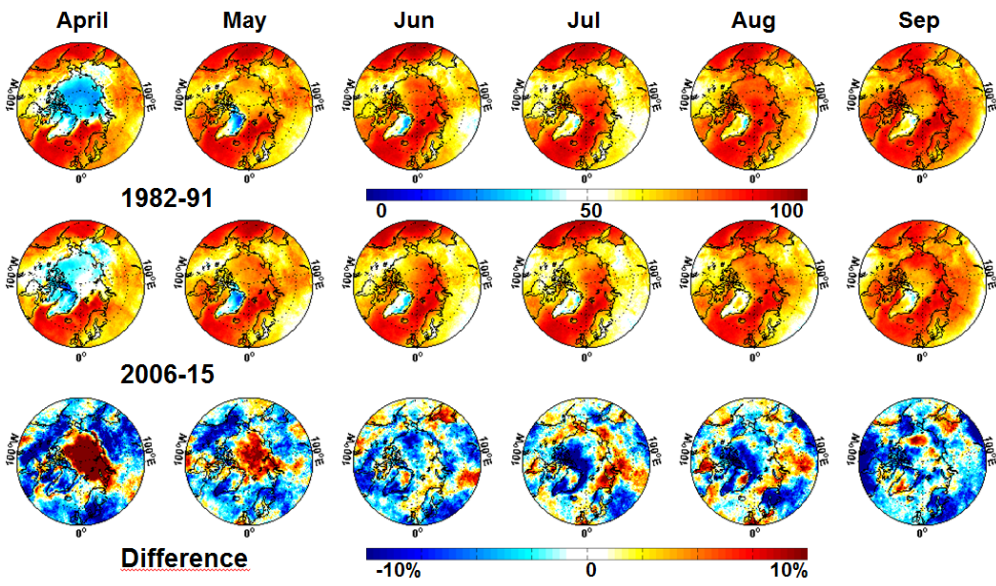
2

3 | Figure 154: Arctic summer season mean surface albedo for the first CLARA-A2 decade (1982-1991, upper
4 | panel) compared to the last decade (2006-2015, middle panel). Difference plot (last minus first decade)
5 | shown in the lower panel. All values shown as %.

6

7

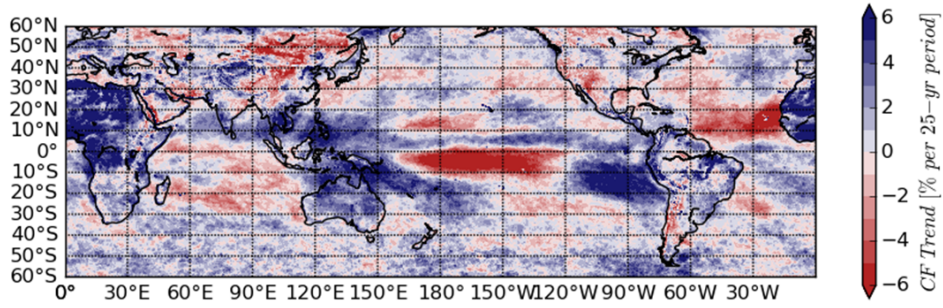
1
2
3
4



5
6
7
8
9
10
11
12

Figure 165: Arctic summer season mean cloudiness for the first CLARA-A2 decade (1982-1991, upper panel) compared to the last decade (2006-2015, middle panel). Difference plot (last minus first decade) shown in the lower panel. All values shown as %.

1
2
3



4
5 | **Figure 176:** Average 25-year trend in cloud cover (%) for low and middle latitudes calculated on the basis
6 | of the average annual trend from CLARA-A2 in the period 1982-2015.
7 |

|

Final reply to Mike Foster's review of the ACPD paper

” CLARA-A2: The second edition of the CM SAF cloud and radiation data record from 34 years of global AVHRR data”

by

Karl-Göran Karlsson et al.

Repeating general statement:

The article is generally well written and organized. The subject matter represents a great deal of work and a significant contribution to the cloud climate community.

That said there are ways I think the article could be improved. There is little discussion and few figures comparing CLARA-A1 to CLARA-A2, which I think makes it more difficult to understand the location and magnitude of improvements. I also think some of the changes could be described in more detail. Specific comments are below.

Reply:

We thank the reviewer for this positive evaluation. In the reply to the specific comments we will outline how we plan to better illustrate the changes and improvements of CLARA-A2 compared to CLARA-A1.

In the following the specific review comments are commented and reference is made to the resulting changes in the revised manuscript (with line numbers taken from the Word document prepared in track change mode).

Repeating specific comment 1:

Section 4: There are lists of specific tasks performed for GAC data pre-processing, histogram, and albedo products. The cloud masking changes are less clear. A list of specific changes might help this. For example, P5 L22 states “Cloud detection during Polar day conditions over snow- and ice-covered surfaces has been optimized, and falsely-detected clouds during Polar night conditions have been largely removed.” How was this done? It might also help to show specific examples – a comparison scene of cloud detection over semi-arid regions for CLARA-A1 and CLARA-A2 would be one possibility.

Reply:

- A list providing more details of the cloud masking algorithm changes will be added.
- For the specific question on cloud detection improvements in the polar regions we can say that we have systematically used CALIPSO cloud observations to identify when in particular falsely-detected clouds occur and with this information we have been able to reduce this problem considerably. For the polar night the focus has been on the latter rather than to improve polar cloud detection further since it is clear that AVHRR cloud detection capabilities during the polar night is already seriously limited. For daytime conditions the CALIPSO information has contributed to a better cloud discrimination over snow- and ice-covered surfaces. We will add this to the discussion in the text.
- Examples of changed results over semi-arid regions will be added.

Final modification of manuscript:

The text has been modified on **page 5 lines 17-36** and **page 6 lines 1-12** in the revised manuscript. A list has been added with more details on the algorithm improvements. Finally, a new Figure 2 has been added illustrating the changes in cloud amounts between CLARA-A2 and CLARA-A1 over the African continent, in particular highlighting the changes over semi-arid regions. In connection to this, two new references (Sun et al., 2015 and Sanchez-Lorenzo et al., 2017) have been added where the semi-arid problem for CLARA-A1 has been highlighted earlier.

Regarding the new Figure 2 one can see that the most remarkable changes are the removal of false-clouds over semi-arid areas (e.g. Sahel and parts of southern Africa) and an increase in the number of detected clouds over pure desert areas and vegetated areas. This leads to quite large changes in the cloud distribution over Africa. However, CALIPSO-based validation results in Figure 4 largely support the updated distribution given by CLARA-A2, thus we believe that we now have a much more realistic cloud distribution over Africa (and globally).

Repeating specific comment 2:

Similarly there is little description of the changes to CTO retrieval. Would it be possible to include a little more detail as to what modifications were made to allow successful retrievals to jump from 70% to 97%?

Reply:

- We will add more details. Basically, the improvement has resulted from applying more physically sound constraints to the iterations.

Final modification of manuscript:

Text has been modified on **page 8 lines 8-10**.

Repeating specific comment 3:

There is not a lot of discussion of how the changes compare to CLARA-A1 (other than Figure 2). I think it would be helpful to include CLARA-A1 data in a few of the comparison figures against PATMOS-x and MODIS (and maybe have a Htrate panel for CLARA-A1 in Figure 3). Figures 7, 9 and 11 seem like good candidates for this.

Reply:

- We will consider adding more CLARA-A1 results, if possible. However, notice that no CLARA-A1 results have ever been produced for the period 2010-2015. Thus, since results in Figure 3 can only be visualised if having enough CALIPSO collocations (i.e., covering the full period 2006-2015) the specific request for that figure cannot be fulfilled. However, some inter-comparison results were produced for the period 2006-2009 and we can add this to the text (and a table).
- For Figures 7 and 11 we see no problem in also including CLARA-A1 results. Figure 9 needs some further consideration.

Final modification of manuscript:

Figures 7, 9 and 11 have now been complemented with CLARA-A1 results. However, notice that new figure numbers are Figure 8, Figure 10 and Figure 12 (which is a consequence of the inclusion of a new Figure 2).

Statements commenting these additional CLARA-A1 results can be found in the revised manuscript:

Figure 8: **page 9, lines 7-19.**

Figure 10: **page 10, lines 11-17.**

Figure 12: **page 11, lines 32-38 + page 12, lines 1-9.**

To notice is also the inclusion of a new Table 2 with inter-comparisons of CLARA-A1 and CLARA-A2 results for the same reference dataset from CALIPSO-CALIOP. Modified text about this can be found on **page 6 lines 21-30.**

Repeating specific comment 4:

Section 7: The comparison against Norris et al. 2016 seems superficial, even by the preliminary standard defined in the manuscript. It is difficult to come to any conclusions based on the single figure 16. A linear regression to remove the ENSO signal might shed some light on this.

Reply:

- We agree that results do not allow firm conclusions, which we also wrote clearly (this should only be seen as a demonstration of what can be studied using the data record). However, to claim that result would be superficial is a too strong statement. We just repeated the study (or parts of the study) in the Norris et al. 2016 paper to see what happens if we add another 7 years to the 27 years that they studied. There are obviously differences but also similarities so it is clear that it is difficult to find very clear conclusions. However, the indication that the cloud changes seen by Norris et al., 2016 for mid- and high-latitudes are maybe not as clear in our study despite having added several years (which should give better prospects of finding a long-term trend) would actually call for further and deepened studies here. For this reason we still think this addition to the paper is interesting.

The recommendation to remove the ENSO signal by a linear regression is questionable. Firstly, this was not done by Norris et al. 2016 in the original study and, secondly, a possible climate change signal could actually also mean a changed behaviour of the frequency and amplitude of ENSO signals. Thus, it would be dangerous to assume a static ENSO behaviour.

In conclusion, we still think that this section adds something to the

scientific discussion and that its presence could help trigger deeper studies about the specifically mentioned topics.

Final modification of manuscript:

We decided to keep Section 7 in the revised manuscript, even if this leads to a significant extension in the length of the paper (considering all other changes). The main reason is that we are keen on seeing more work being done on the exemplified applications so we really want to encourage this.

We removed the statement that results are preliminary and we instead underlined that the provided results are results directly derived from the CLARA-A2 data record (**page 14, lines 3-7**). We also emphasized again (**page 15, lines 4-8**) the importance and significance of having a longer time series of data (7 additional years) when repeating the study by Norris et al., (2016). However, we also repeated in both example cases that further in depth studies are needed here to evaluate the full impact of the results (**page 14, lines 29-31**).

See also discussion in final reply to Anonymous Referee 1.

Finally, we have also added the correct reference to the paper by Norris et al., (2016) which unfortunately was missing in the first version of the manuscript.

Repeating specific comment 5:

Figures 3 and 4 – the red-blue colorbar is usually used for temperature or something with positive and negative values. Also it is a little difficult to differentiate the value of Hitrate for higher values.

Reply:

We don't fully understand this comment. What we show is definitely something related to positive and negative values even if it expressed in a relative sense. Blue colours define poor validation scores and red values good validation scores. For example, in the case of Figure 4 the 50 % level of probability of detection must be considered as a critical negative case (i.e., here we only detect 50 % of all clouds). However, we admit that the choice of the intermediate point (i.e., when blue changes to red), which could be interpreted as the point where we go from bad to good results, is rather arbitrarily chosen. We will consider changing to a better color representation.

Final modification of manuscript:

We have introduced new color tables for the two figures (now renamed to Figure 4 and Figure 5). We basically avoided using the red and blue colours in this context.

Notice also the additional explanatory text about the used dataset for producing Figures 4 and 5 (**Page 6, lines 37-39 + Page 7, line 1**).

Repeating specific comment 6:

P4 – Are observations under twilight conditions excluded for all products, or just for the monthly averages?

Reply:

All cloud products except Cloud Physical Products (COT, REF, LWP, IWP) are based on all observations. The CPP exceptions are explained by the needed access to daytime visible channel data for the retrieval methods.

The exclusion of twilight data is restricted to complementary sub-layers to the cloud amount (CFC) and cloud phase (CPH) products. Thus, the main CFC and CPH products are based on all observations but in addition a user can choose to look also at CFC and CPH sub-layers showing results exclusively at daytime or exclusively at nighttime. When defining these two sub-layers no data under twilight conditions was used. These sub-layers are available for both daily and monthly CFC products. For the CPH product the standard product is complemented with a daytime product (no night-time product is prepared).

The description in the text is not correct and we will clarify.

Final modification of manuscript:

The text has been modified in three locations in the text:

1. **Page 4, lines 25-31** – introducing the idea of complementary day/night information.
2. **Page 5, line 13** – specifying for CFC
3. **Page 8, lines 32-34)** – specifying for CPP and CPH

To repeat, the exclusion of twilight data only affects the CFC and CPH products yielding two complementary daytime and nighttime products in addition to the standard CFC product based on all data plus one complementary daytime CPH product.

Repeating specific comment 7:

P6 L7 – I don't understand this explanation. Is there perhaps a citation showing that the dry sub-tropical regions with decreased Hitrate are areas where sub-pixel scale clouds frequently occur?

Reply:

We are not certain what the problem is here (the reference to Page 6 Line 7 is not very specific). But if the question is only about the statement on the low Hitrate for dry-subtropical regions we can say the following:

Marine stratocumulus and cumulus clouds are dominant clouds over most marine ocean surfaces in the tropics and in the sub-tropics (if not being too close to the ITCZ). The frequency and the extent of clouds in these regions have definitely links to the size of the clouds. In the centre of sub-tropical anticyclones or highs cumulus clouds are mostly occurring as individual small-scale clouds (cumulus humilis + cumulus mediocris + cumulus congestus) with limited horizontal and vertical extent and with low frequency. Many of those cloud elements have sizes significantly smaller than the AVHRR GAC pixel (e.g., cumulus humilis or broken stratocumulus). However, away from the centre the number of clouds and their extent normally increases gradually with the distance from the centre. At some point the dominant cloud type may also change from individual cumulus clouds to stratocumulus clouds with larger horizontal extensions. We also often see a transition from cumulus clouds in open cell formation to closed cell formation. The cloud distribution is also affected by ocean current effects so that regions with colder ocean surfaces may lead to almost overcast stratocumulus conditions. Good examples here are the ocean waters outside (to the west of) Namibia and Peru. What we claim here is that, since the occurrence of really small and exclusive (i.e., not accompanied by larger scale clouds) cumulus cloud elements is more likely for the reasons explained earlier in the central regions of the sub-tropical highs, the risk of encountering matchup problems between AVHRR GAC pixels (with 5 km dimensions) and CALIPSO observations (with 300 m width FOVs) is higher here than outside of the central portions of the sub-tropical highs. We think that this is supported by the pattern in the Hitrate plots which highlights the decrease in Hitrate over typical positions of the sub-tropical highs. In conclusion, we believe that the reduced scores over sub-tropical high regions must be related to a higher relative frequency of small (sub-pixel scale) cloud elements among all

existing clouds leading to both enhanced CALIPSO collocation problems and to some extent also to a less efficient cloud detection.

The main problem here is that, neither the actual AVHRR GAC measurement (formed by sub-sampling only every fourth original 1 km resolution AVHRR scanline), nor the CALIOP observation (a narrow 330 m sampling in 15 measurements/lidar shots), is capable of covering the nominal GAC FOV more than to 10-20 %. Furthermore, they observe different portions of the GAC FOV since the AVHRR and CALIOP observation arrays are almost perpendicular. So when cloud element sizes go below 5 km the likelihood increases that the cloud is not observed simultaneously anymore in the two datasets. This explains the decreased validation scores.

The same thing could also happen over land areas with a high frequency of small-scale cloud elements but we think that the existence of more vigorous and widespread convection over land areas (as an effect of more heterogeneous surface conditions) might reduce this effect. However, we notice also low values over the eastern part of South-America and in eastern Africa which also could be linked to a high frequency of small cumulus cloudiness during periods of higher atmospheric stability.

To really prove this hypothesis is difficult (requires extensive high-resolution measurements over long periods) so we suggest that we modify the text in a way that we express this as a possible explanation rather than as a well-established truth. Maybe reliable global cloud-size statistics can eventually be collected from CALIPSO observations to reveal the answer, given that we could possibly be given a few more years of CALIPSO satellite operations.

Final modification of manuscript:

We have added a few clarifying sentences in the text (**Page 7, lines 1-17**) based on the more extensive reply above.

Repeating specific comment 8:

Figure 12 – Hard to differentiate between blue and black dots

Reply: We will try to improve the visibility here.

Final modification of manuscript:

The figure has been updated (new name is Figure 13). Dots have been made bigger and the blue colour has been changed to red.

Technical Corrections:

P2 L10 – ‘lined out’ should be ‘outlined’ P2 L18 – ‘already’ is unnecessary and can be removed P2 L37 – the grammar and use of semicolon in this sentence is odd – consider rewording P3 L1 – Sentence beginning with "Additionally, orbital drift..." is awkward. Consider rewording P3 L9 – incorrect usage of the word ‘spurious’ P5 L13 “is using” should be “uses” P5 L26 – Should be “spurious” or “false” cloud, not both.

Reply:

We will certainly correct this. Thanks for the suggestions.

Final modification of manuscript:

All technical corrections are implemented.

Final reply to Referee 1's review of the ACPD paper

” CLARA-A2: The second edition of the CM SAF cloud and radiation data record from 34 years of global AVHRR data”

by

Karl-Göran Karlsson et al.

Repeating general statement:

The manuscript "CLARA-A2: The second edition of the CM SAF cloud and radiation data record from 34 years of global AVHRR data" by K.-G. Karlsson et al. fits the scope of the journal and deserves to be considered for publication after some changes are made.

The paper is reasonably well written and understandable. Results and figures are provided with a sufficient quality.

Reply:

We thank the reviewer for this positive evaluation. We will reply to the specific comments below.

In the following the specific review comments are commented and reference is made to the resulting changes in the revised manuscript (with line numbers taken from the Word document prepared in track change mode).

Repeating specific comment 1:

The manuscript contains several statements on the improvements of CLARA-A2 with respect to the previous version CLARA-A1. While this is fine and informative for potential users, such improvements are not sufficiently documented. Figure 2 presents a comparison, but there is not much more than this in the rest of the paper. The authors should consider adding some more material.

Reply:

Yes, we will present more inter-comparisons with CLARA-A1 results. For example, we did cloud product inter-comparisons based on CALIPSO observations for both data records for the period 2006-2009 which were not reported in the manuscript. We will add some of these results. Also for other CLARA-A2 parameters we will try to add more inter-comparisons against CLARA-A1. For example, Figures 7 and 11 will be updated with CLARA-A1 results.

Final modification of manuscript:

A new table (Table 2) has been added showing inter-comparisons of CLARA-A1 and CLARA-A2 results being compared to a reference dataset of CALIPSO observations. Corresponding text in the manuscript is found on **page 6, lines 21-30**.

Figures 7, 9 and 11 have now been complemented with CLARA-A1 results. However, notice that new figure numbers are Figure 8, Figure 10 and Figure 12 (which is a consequence of the inclusion of a new Figure 2).

Statements commenting these additional CLARA-A1 results can be found in the revised manuscript:

Figure 8: **page 9, lines 7-19**.

Figure 10: **page 10, lines 11-17.**

Figure 12: **page 11, lines 32-38 + page 12, lines 1-9.**

The text has also been modified further (**page 5, lines 17-36 + page 6, lines 1-12**) in the revised manuscript. A list has been added with more details on the algorithm improvements since CLARA-A1. Finally, a new Figure 2 has been added illustrating the changes in cloud amounts between CLARA-A2 and CLARA-A1 over the African continent, in particular highlighting the changes over semi-arid regions. In connection to this, two new references (Sun et al., 2015 and Sanchez-Lorenzo et al., 2017) have been added where the semi-arid problem for CLARA-A1 has been highlighted earlier.

Repeating specific comment 2:

The Section 7 seems to me a bit too quick. The analyses presented in the section (chiefly the one on the change of cloud conditions in the Arctic and Northern Hemisphere) are admittedly conducted as a very preliminary effort. However, even adopting this perspective, the material and figures are integral parts of the paper and would require more studies in order to be published. I am not in favour of including this part. Perhaps the space saved could be effectively allocated to address the previous point of this review.

Reply:

The recommendation from the reviewer to not present this part is obviously strong and should be obeyed.

At the same time, we added this section because we wanted to point out with some examples a couple of application areas which we found especially interesting. Also, we wanted the manuscript to include a little bit more of scientific discussion to justify it better in the ACP context (we have heard the argument that there are other journals more suitable for sheer descriptions of new data records). Thus, before taking the step to remove the section we want to have the opportunity to provide some more arguments (including the previously

mentioned). After having provided that, we will wait for a final recommendation from the reviewer.

The Arctic surface albedo plots were kind of natural to include with respect to the ongoing concern about the observed reduction of summertime Arctic ice coverage. The new thing here was that it would in our opinion be interesting to also relate it to changes in Arctic cloudiness. Both parameters are available in CLARA-A2 and we just wanted to point that out. The cloud results are certainly not as conclusive as the surface albedo plots but this is nevertheless an interesting piece of information pointing out that ice melting processes do not seem to be directly and highly correlated with changes in cloud cover. The results as such cannot be considered as preliminary (the choice of word here is unfortunate) since they have been produced in exactly the same manner as the surface albedo results, i.e., by use of all monthly averages over the studied period. So, these are final CLARA-A2 results and not preliminary ones. However, this is only a first observation based on monthly and yearly averages which could be complemented by more detailed studies also including additional information (e.g. circulation patterns, warm/cold advection conditions, cloud types, etc) to enable a deeper analysis.

Regarding the other example (about global 25-year average trends of cloudiness) we have similar arguments. We just repeated the study (or parts of the study) in the Norris et al. 2016 paper to see what happens if we add another 7 years to the 27 years that they studied. There are obviously differences but also similarities so it is clear that it is difficult to find very clear conclusions. However, the indication that the cloud changes seen by Norris et al., 2016 for mid- and high-latitudes (and which were specifically high-lighted in the conclusions) are maybe not as clear in our study despite having several additional years which would reasonably give better prospects of finding a long-term trend. This would actually call for further and deepened studies here. For this reason we still think this addition to the paper is interesting.

We'll await a final recommendation on the potential removal of Section 7. If that recommendation stands firm we hope that we can at least use the figures (both or one of them) to further illustrate the product groups of clouds and surface albedo in sections 4 and 5.

Final modification of manuscript:

We decided to keep Section 7 in the revised manuscript, even if this leads to a significant extension in the length of the paper (considering all other changes). The main reason is that we are keen on seeing more work being done on the exemplified applications so we really want to encourage this.

We removed the statement that results are preliminary and we instead underlined that the provided results are results directly derived from CLARA-A2 data record (**page 14, lines 3-7**). We also emphasized again (**page 15, lines 4-8**) the importance and significance of having a longer time series of data (7 additional years) when repeating the study by Norris et al., (2016). However, we also repeated in both example cases that further in depth studies are needed here to evaluate the full impact of the results (**page 14, lines 29-31**).

Finally, we have also added the correct reference to the paper by Norris et al., (2016) which unfortunately was missing in the first version of the manuscript.

Repeating specific comment 3:

The black/blue colour choice of the dots in the figure (Figure 12) makes them difficult to spot.

Maybe a black/red choice would do the job much better.

Reply:

Figure 12 will be revised to increase readability.

Final modification of manuscript:

The figure has been updated (new name is Figure 13). Dots have been made bigger and the blue colour has been changed to red.